Linear and Nonlinear Statistical Response Theories with Prototype Applications to Sensitivity Analysis and Statistical Control of Complex Turbulent Dynamical Systems

Andrew J. Majda [a] and Di Qi [a]

June 29, 2019

[a] Department of Mathematics and Center for Atmosphere and Ocean Science, Courant Institute of Mathematical Sciences, New York University, New York, NY 10012

Abstract

Statistical response theory provides an effective tool for the analysis and statistical prediction of high-dimensional complex turbulent systems involving a large number of unresolved unstable modes, for example, in climate change science. Recently, the linear and nonlinear response theories have shown promising developments in overcoming the curse-of-dimensionality in uncertain quantification and statistical control of turbulent systems by identifying the most sensitive response directions. We offer an extensive illustration of using the statistical response theory for a wide variety of challenging problems under a hierarchy of prototype models ranging from simple solvable equations to anisotropic geophysical turbulence. Directly applying the linear response operator for statistical responses is shown to only have limited skill for small perturbation ranges. For stronger nonlinearity and perturbations, a nonlinear reduced-order statistical model reduction strategy guaranteeing model fidelity and sensitivity provides a systematic framework to recover the multiscale variability in leading order statistics. The linear response operator is applied in the training phase for the optimal nonlinear model responses requiring only the unperturbed equilibrium statistics. The statistical response theory is further applied to the statistical control of inherently high dimensional systems. The statistical response in the mean offers an efficient way to recover the control forcing from the statistical energy equation without the need to run the expensive model. Among all the testing examples, the statistical response strategy displays uniform robust skill in various dynamical regimes with distinct statistical features. Further applications of the statistical response theory include the prediction of extreme events and intermittency in turbulent passive transport and a rigorous saturation bound governing the total statistical growth from initial and external uncertainties.

1 Introduction

Complex turbulent dynamical systems appear in a wide variety of areas in science and technology. Typical examples can be found in interacting physical, biological, and social processes across a huge range of time and spatial scales of overwhelming complexity [45, 65, 72, 63, 71]. Such turbulent systems are usually characterized by an irreducible high-dimensional phase space and a large number of instabilities that move energy across the scales. Instabilities due to the positive Lyapunov exponents as well as the external forcing excitations lead to rapid growth of small perturbations in the high dimensional space [20, 45, 39]. A statistical description with model reduction strategies for the state variables becomes necessary. One example of practical significance [77, 23, 42, 64] is the prediction of climate change from external forcing perturbations such as the impact from increased carbon dioxide. Mitigation of such effects from the climate change also requires effective control strategies [38, 8] which form another set of challenging problems.

Linear response theory together with the fluctuation dissipation theorem (FDT) offers a promising tool for the statistical quantification and prediction of turbulent systems [40, 35]. It predicts statistical averages of the functionals of interest (the *response*) requiring only the unperturbed equilibrium statistical information (the *climate*). The potential validity of the linear response theory has been widely investigated in both theories [29, 43, 6, 25] and numerical algorithms [1, 26, 27, 11] through a variety of test models and techniques. In the study of coarse-grained large-scale variability in climate change, the FDT using linear response operators provides a direct leading-order approximation of the statistical responses in a

unified fashion valid for multiple climate change scenarios with different forcing, dissipation, and other parameters without the need to repeatedly run the complex climate model with various perturbations [35, 46].

Despite the many successes in the linear response theory, this method is significantly hampered by the fundamental constraint within small perturbation amplitudes. It is shown that the linear statistical predictions are usually accurate for the mean responses with near-Gaussian statistics, while the performance for predicting the variance responses can quickly deteriorate in some systems as the forcing perturbation as well as the non-Gaussianity grows large [22, 53, 25]. To overcome the limited range of skill in the linear response prediction, new statistical nonlinear response theories and methods have been proposed and become one main theme in the contemporary research [45, 74, 26, 73, 24]. A systematic methodology has been proposed [39, 53] for capturing the principal statistical nonlinear responses to changes in forcing using statistical reduced-order models. A precise strategy to calibrate the imperfect model error and improve the prediction skill in response to anisotropic perturbations (such as the climate change) is developed relying on the information-theoretic framework [40, 51, 33], so that the overwhelming computational demands in Monte-Carlo simulations in a high dimensional space are avoided.

In this paper, we review the linear and nonlinear statistical response theories with a focus on the variety of important and effective applications in uncertainty quantification (UQ) and control of turbulent complex systems. A hierarchy of dynamical models with increasing complexity (see in Section 2.2) is proposed to illustrate the representative features of the statistical response theory and the related information-theoretic framework. The key problems to be discussed include the following interrelated topics which have crucial applications to many realistic systems from nature.

Approximating linear response operators with Gaussian and non-Gaussian equilibrium statistics

The practical computation of the linear response operator for FDT requires proper characterization for the usually inaccessible equilibrium statistical distribution of the unperturbed system. A first approximation is through the quasi-Gaussian closure (qG-FDT) proposed first by Leith [35], and has been generalized and improved for both mean and variance responses with many successful applications [46, 51, 21]. To compute the linear response operators from a strongly non-Gaussian equilibrium state, a kicked response of the unperturbed system is proposed [40, 53] where the higher moment feedbacks are better incorporated in an efficient way. The extent of skills in the linear response theory is illustrated under the explicit solvable model [46] and the two-layer Lorenz '96 system [34] (in Section 3.2).

Improving the prediction skill of nonlinear responses through the information-theoretic framework

The nonlinear response theory aims to obtain the statistical estimates of changes in mean and variance for key quantities in the nonlinear responses to external forcing or uncertain initial state. Reduced-order statistical models are constructed for the most sensitive subspace. The linear response operator offers a precise systematic framework to improve imperfect model sensitivity through measuring the information error in the training phase using only unperturbed statistics. Empirical information theory [33, 40] offers an unbiased invariant metric for calibrating the model error in the response operators, and systematically improves model sensitivity in a unified way with model fidelity [17, 50]. Besides, a statistical energy principle [44] is adopted to improve the imperfect model prediction skill by offering the total energy profile without increasing the computational cost too much.

The basic ideas in the construction of the reduced-order statistical model are first illustrated using the triad system with quadratic energy transfer (in Section 3.3). The improved skill in the nonlinear prediction is discussed in detail using the prototype topographic barotropic model describing the interactive motion of large-scale mean flow and small-scale vortical modes [68] (in Section 4). The model displays a rapid change of directions in the large scale jets sensitive to external perturbations. It is shown that the principal statistics in first and second moments including the shifting jet directions can be captured with desirable accuracy and efficiency using a reduced-order model with only three resolved modes. Besides, a rigorous saturation bound [70] is derived for quantifying the total changes in the mean fluctuation and variance due to initial and external perturbations.

Controlling inhomogeneous responses using statistical functional responses in high dimension

The control of turbulent systems concerns the optimal course of actions to drive the states of interest to a desired final condition with a minimum cost. Solving the control problem in highly turbulent systems directly is always challenging due to the large instabilities and strong nonlinear exchange of energy among different scales [8, 16]. Statistical response theory provides an alternative approach for controlling the a statistical scalar identity [54, 55] where the instability due

to the symmetric nonlinear interactions can be circumvented. Simple autocorrelation functions can be approximated in an explicit form to represent the linear mean response, so that the specific control forcing is determined offline without the need to run the complex high-dimensional system to get the responses. The topographic barotropic flow is used again to demonstrate the control skill in geophysical turbulence with non-Gaussian statistics and instabilities (in Section 5).

Predicting extreme events and tracer intermittency in passive scalar turbulence

Extreme events represented by non-Gaussian fat-tails in passive tracer distributions are a universal feature in observation, experiments, and numerical simulations [19, 62, 52]. As another effective application of the response theory, the capability of using stochastic reduced-order models to capture crucial tracer statistical features is achieved using more tractable linear Gaussian stochastic models with optimization for its linear response functionals [66, 69]. The same systematic model reduction procedure for the statistical response is adopted. The passive scalar simulation is tested using a two-layer baroclinic turbulent flow which can generate various representative atmosphere and ocean regimes with jets and vortices (in Section 6).

In the structure of this paper, a general overview of the linear and nonlinear statistical theories is given in Section 2 in company with the general model formulation. Using simple prototype models, the accuracy of various statistical response functionals under the several proposed approximation methods is compared in Section 3. The linear and nonlinear response theories are applied to more practical geophysical turbulence model in Section 4 to show their practical skills. Further important applications of the statistical response theory for effective statistical control of turbulent system and prediction of extreme events in passive tracer turbulence are discussed in Section 5 and Section 6 separately. A summary is given in Section 7 discussing the accuracy and extent of applications of the linear and nonlinear response theories.

2 Statistical Response Theory and Algorithms for Computing the Linear Response Operators

In this section, we review the statistical formulation for the general complex turbulent systems, and display the main conclusions from the linear response theory. Efficient algorithms to compute the response operators are also described.

2.1 A review of the general complex turbulent systems

One representative feature in complex turbulent dynamical systems from nature is the nonlinear energy conserving interaction that transports energy from the unstable subspace to stable one where the energy is strongly dissipated, resulting in a final statistical steady state in equilibrium. The general abstract formulation of the turbulent dynamical systems is proposed [45, 39] for the state variable of interest $\mathbf{u} \in \mathbb{R}^N$ in a high-dimensional phase space

$$\frac{d\mathbf{u}}{dt} = (\mathcal{L} + \mathcal{D})\mathbf{u} + B(\mathbf{u}, \mathbf{u}) + \mathbf{F}(t) + \boldsymbol{\sigma}(t)\dot{\mathbf{W}}(t; \omega). \tag{2.1}$$

On the right hand side of the above equation (2.1), the first two components, $(\mathcal{L} + \mathcal{D})\mathbf{u}$, represent linear dispersion and dissipation effects, where $\mathcal{L}^* = -\mathcal{L}$ is an energy-conserving skew-symmetric operator; and $\mathcal{D} < 0$ is a negative definite operator. The nonlinear effect in the dynamical system is introduced through a quadratic form, $B(\mathbf{u}, \mathbf{u})$, that satisfies the conservation law and the Liouville property, so that

$$\text{Energy Conservation}: \quad \mathbf{u} \cdot B(\mathbf{u}, \mathbf{u}) = \sum_{j=1}^{N} u_j B_j(\mathbf{u}, \mathbf{u}) \equiv 0, \tag{2.2a}$$

$$\text{Liouville Property}: \quad \text{div}_{\mathbf{u}} B(\mathbf{u}, \mathbf{u}) = 0. \tag{2.2b}$$

Besides, the system is subject to external forcing effects that are decomposed into a deterministic component, $\mathbf{F}(t)$, and a stochastic component represented by a Gaussian random process, $\boldsymbol{\sigma}(t)\dot{\mathbf{W}}(t; \omega)$. It needs to be emphasized that in many situations $\mathbf{F}$ might be inhomogeneous and introduce anisotropic structures into the system, and $\boldsymbol{\sigma}(t)\dot{\mathbf{W}}(t; \omega)$ might further alter the energy structure in the fluctuation modes.

The internal instability and the stochastic random forcing in the turbulent system (2.1) require a statistical description for the state variable $\mathbf{u}$. Assuming that the stochastic white noise is written in the Ito sense, the probability density function $p(\mathbf{u}, t)$ can be found directly from the solution of the associated Fokker-Planck equation (FPE)

$$\frac{\partial p}{\partial t} \equiv \mathcal{L}_{\mathrm{FP}} p = -\mathrm{div}_{\mathrm{u}} \left[B(\mathbf{u}, \mathbf{u}) p + (\mathcal{L}\mathbf{u} + \mathcal{D}\mathbf{u}) p \right] + \frac{1}{2} \mathrm{div}_{\mathbf{u}} \nabla \left(\sigma \sigma^T p \right). \tag{2.3}$$

The unperturbed climate is associated with the equilibrium density function $p_{\mathrm{eq}}(\mathbf{u})$ that satisfies the invariant equation $\mathcal{L}_{\mathrm{FP}} p = 0$. Usually, we are interested in the statistics in some functional $A(\mathbf{u})$ defined by the expectation according to the density function

$$\langle A \rangle_p = \int A(\mathbf{u}) p(\mathbf{u}) d\mathbf{u}, \quad \langle A \rangle_{\mathrm{eq}} = \int A(\mathbf{u}) p_{\mathrm{eq}}(\mathbf{u}) d\mathbf{u},$$

where $\langle A \rangle_p$ is the general expectation while $\langle A \rangle_{\mathrm{eq}}$ gives the unperturbed equilibrium statistics. There are important turbulent dynamical systems where the FPE can be solved even with large dimension and highly non-Gaussian statistics [15, 14]. However, it is still generally a challenging task for directly solving the FPE system (2.3) especially when the dimensionality of the system becomes large.

2.1.1 A statistical formulation of general turbulent systems

Due to the turbulent features of the general systems (2.1) and the high computational cost to solve the Fokker-Planck equation (2.3), it is often useful to derive a dynamical formulation for the evolution of key statistical moments. To achieve this, we rewrite the stochastic field $\mathbf{u}$ in a finite-dimensional representation consisting of a fixed-in-time, N-dimensional, orthonormal basis $\{\mathbf{e}_i\}_{i=1}^N$

$$\mathbf{u}(t) = \bar{\mathbf{u}}(t) + \sum_{i=1}^N Z_i(t; \omega) \mathbf{e}_i, \quad R_{ij} = \langle Z_i Z_j^* \rangle, \tag{2.4}$$

where $\bar{\mathbf{u}}(t) = \langle \mathbf{u}(t) \rangle$ represents the statistical expectation of the model state mean response (we use the angled bracket $\langle \cdot \rangle$ to represent the ensemble average), i.e. the mean field; and $\{Z_i(t; \omega)\}$ are stochastic coefficients (with ω to denote a random process) measuring the fluctuation processes along each model direction $\mathbf{e}_i$. In most of the situations, we are interested in the time evolution of the mean state $\bar{\mathbf{u}}$ and the covariance R charactering the variability among different modes.

By taking the statistical (ensemble) average over the original equation (2.1) and using the mean-fluctuation decomposition (2.4), the *evolution equations of the mean state $\bar{\mathbf{u}}$ and the covariance matrix R* are given by the following dynamical equations

$$\frac{d\bar{\mathbf{u}}}{dt} = (L + D) \bar{\mathbf{u}} + B(\bar{\mathbf{u}}, \bar{\mathbf{u}}) + \sum_{i,j} R_{ij} B(\mathbf{e}_i, \mathbf{e}_j) + \mathbf{F}, \tag{2.5a}$$

$$\frac{dR}{dt} = L_u(\bar{\mathbf{u}}) R + R L_u^*(\bar{\mathbf{u}}) + Q_F + Q_\sigma. \tag{2.5b}$$

with $R = \langle \mathbf{Z}\mathbf{Z}^* \rangle$ the second-order covariance matrix of the stochastic coefficients $\mathbf{Z} = [Z_1, \cdots, Z_N]^T$. The detailed derivation of the above equations follows that standard procedure and can be found in [39, 74]. The explicit forms of the operators in the covariance equation are summarized as follows organized from different order statistics:

i) the quasi-linear operator $L_u(\bar{\mathbf{u}})$ expresses the linear coupling of non-normal dynamics (effect due to $\mathcal{L}$) and energy dissipation (effect due to $\mathcal{D}$), as well as the energy transfers between the mean field and the stochastic modes (effect due to B)

$$\{L_u\}_{ij} = [(\mathcal{L} + \mathcal{D}) \mathbf{e}_j + B(\bar{\mathbf{u}}, \mathbf{e}_j) + B(\mathbf{e}_j, \bar{\mathbf{u}})] \cdot \mathbf{e}_i; \tag{2.6a}$$

ii) the positive definite operator Q_σ expresses energy injection from the external stochastic forcing

$$\{Q_\sigma\}_{ij} = \sum_k (\mathbf{e}_i \cdot \sigma_k)(\sigma_k \cdot \mathbf{e}_j); \tag{2.6b}$$

4

iii) the nonlinear energy flux Q_F expresses nonlinear energy exchanges between different fluctuation modes due to non-Gaussian statistics (or nonlinear terms) modeled through third-order moments

$$\{Q_F\}_{ij} = \sum_{m,n} \langle Z_m Z_n Z_j \rangle B(\mathbf{e}_m, \mathbf{e}_n) \cdot \mathbf{e}_i + \langle Z_m Z_n Z_i \rangle B(\mathbf{e}_m, \mathbf{e}_n) \cdot \mathbf{e}_j. \tag{2.6c}$$

We stress that the energy conservation property of the quadratic operator B from (2.2a) is inherited in the statistical equations by the matrix Q_F since the energy conservation property for the fluctuation state $\mathbf{u}'$ yields

$$\mathrm{tr}(Q_F) = 2 \sum_i \sum_{m,n} \langle Z_m Z_n Z_i \rangle B(\mathbf{e}_m, \mathbf{e}_n) \cdot \mathbf{e}_i = 2B(\mathbf{u}', \mathbf{u}') \cdot \mathbf{u}' \equiv 0.$$

The above exact statistical equations for the state of the mean (2.5a) and covariance matrix (2.5b) will be the starting point for the developments in the reduced-order models on UQ methods.

Note that the above procedure by adding higher and higher order moment equations can never construct a closed system. The statistical dynamics for the mean (2.5a) and covariance (2.5b) are not closed due to the inclusion of third-order moments through the nonlinear interactions in Q_F in (2.6c). The basic idea in developing reduced-order schemes concerns proper approximation of this energy flux term Q_F in a simple and efficient manner so that the energy mechanism can be properly modeled for both the transient state and the final equilibrium [39, 45].

2.1.2 A statistical energy identity for turbulent systems

Despite the fact that the exact equations for the statistical mean (2.5a) and the covariance fluctuations (2.5b) are not a closed system, there exists a suitable statistical symmetry so that the total energy in the mean plus the total variance satisfies an energy conservation principle even with the general deterministic and random forcing. Here, we briefly describe the result in the statistical theory developed in [44, 45] about a statistical energy functional for the abstract system (2.1). As we will show in the later sections, this total statistical energy offers a general description about the total responses in the perturbed system and will be play a crucial role in the construction of various nonlinear response and control theories.

For characterizing the total statistical variability in the turbulent system, we consider the statistical mean energy, $\bar{E} = \frac{1}{2} |\bar{\mathbf{u}}|^2 = \frac{1}{2} \bar{\mathbf{u}} \cdot \bar{\mathbf{u}}$, for the total energy in the mean; and the statistical fluctuation energy, $E' = \frac{1}{2} \langle \mathbf{u}' \cdot \mathbf{u}' \rangle = \frac{1}{2} \mathrm{tr} R$, for the total variability in the system. Further, the following symmetries are assumed [44] involving the nonlinear interaction operator B under the orthonormal basis $\{\mathbf{e}_i\}$:

A) The self interactions vanish in the quadratic interaction,

$$B(\mathbf{e}_i, \mathbf{e}_i) \equiv 0, \quad 1 \le i \le N; \tag{2.7a}$$

B) The dyad interaction coefficients vanish through the symmetry,

$$\mathbf{e}_i \cdot [B(\mathbf{e}_j, \mathbf{e}_i) + B(\mathbf{e}_i, \mathbf{e}_j)] = 0, \quad \text{for any } i, j. \tag{2.7b}$$

The above *detailed triad symmetry* guarantees that the nonlinear interaction $B(\mathbf{u}, \mathbf{u})$ will not alter the total statistical energy structure in the system (though the state of the mean and covariance may both changed due to the nonlinear terms in equations (2.5a) and (2.5b)). It can be found satisfied among many systems including the examples shown next. Therefore, we have the following theorem for general turbulent systems [44, 45]:

Theorem 1. *(Statistical Energy Conservation Principle) Under the structural assumptions (2.7a), (2.7b) on the basis $\mathbf{e}_i$, for any turbulent dynamical systems (2.1), the total statistical energy, $\langle E \rangle = \bar{E} + E' = \frac{1}{2} \bar{\mathbf{u}} \cdot \bar{\mathbf{u}} + \frac{1}{2} \mathrm{tr} R$, satisfies the scalar dynamical equation*

$$\frac{d \langle E \rangle}{dt} = \bar{\mathbf{u}} \cdot D\bar{\mathbf{u}} + \bar{\mathbf{u}} \cdot \mathbf{F} + \mathrm{tr}(DR) + \frac{1}{2} \mathrm{tr} Q_\sigma, \tag{2.8}$$

where $\bar{\mathbf{u}}$ and R are the exact solutions from the statistical equations (2.5).

Especially under homogeneous structures, $D = -dI$ and $\mathbf{F} = fI$, the right hand side of the statistical energy equation (2.8) becomes a linear damping on the total energy, $-d \langle E \rangle$, plus the deterministic forcing applying on the homogeneous mean state, $\bar{u}f$, and the stochastic forcing contribution. This implies that the total energy structure (and thus the second-order variance in all the modes) can be determined purely from the first-order mean state by solving a simple scalar equation.

5

2.2 Prototype models for complex turbulent dynamical systems

Many complex turbulent dynamical systems can be categorized into the previous abstract mathematical structure (2.1) satisfying the structural properties (2.2a) and (2.2b). A series of typical prototype models can be found for the investigation of complex turbulent dynamical systems. These qualitative and quantitative models with increasing complexity form a desirable hierarchical set of testing models for various applications in prediction with model error, uncertainty quantification, and state estimation [45, 39, 30].

(A) *The triad system with explicit solution.* The triad model [45, 41] offers an elementary building block of complex turbulent systems with exact solvable solutions. It is a 3-dimensional ODE system with inhomogeneous damping and both deterministic and stochastic forcing terms

$$
\begin{aligned}
\frac{du_1}{dt} &= -d_1 u_1 - L_3 u_2 + L_2 u_3 + B_1 u_2 u_3 + F_1 + \sigma_1 \dot{W}_1, \\
\frac{du_2}{dt} &= L_3 u_1 - d_2 u_2 - \frac{L_1}{\epsilon} u_3 + B_2 u_3 u_1 + F_2 + \sigma_2 \dot{W}_2, \\
\frac{du_3}{dt} &= -L_2 u_1 + \frac{L_1}{\epsilon} u_2 - d_3 u_3 + B_3 u_1 u_2 + F_3 + \sigma_3 \dot{W}_3.
\end{aligned}
\tag{2.9a}
$$

The strategies for constructing reduced-order models are built on this triad model without scale separation $\epsilon = 1$ in [39]. Another interesting set of problems is described in [45] for testing the multiscale dynamics with $\epsilon \ll 1$ and no nonlinearity $B_1 = B_2 = B_3 = 0$. The triad nonlinear stochastic model also offers an unambiguous testbed for the statistical responses in a time-periodic setting [21].

(B) *The one and two-layer Lorenz '96 model.* The original Lorenz '96 (L-96) model is a 40-dimensional ODE system introduced first by Lorenz [36]

$$
\frac{du_j}{dt} = (u_{j+1} - u_{j-2}) u_{j-1} - d u_j + F_j, \ j = 1, \cdots, J = 40.
\tag{2.9b}
$$

It is defined with periodic boundary condition mimicking geophysical waves in the mid-latitude atmosphere. Various representative statistical features can be generated by changing the external forcing values in F [40, 45, 46]. In addition, a two-layer generalization [46, 34] is introduced by coupling the original L-96 model (2.9b) with a second level dynamics

$$
\begin{aligned}
\frac{du_j}{dt} &= (u_{j+1} - u_{j-2}) u_{j-1} - d u_j + F_j - \lambda \sum_k Y_{j,k}, \\
\frac{dv_{j,k}}{dt} &= \frac{1}{\epsilon} v_{j,k+1} \left(v_{j,k-1} - v_{j,k+2} \right) - d_{j,k} v_{j,k} + \lambda u_j,
\end{aligned}
\tag{2.9c}
$$

where $\epsilon > 0$ is the time scale separation parameter and $\lambda > 0$ is the nonlinear coupling parameter. The subindexes $j = 1, \cdots, J$ and $k = 1, \cdots, K$ are for the first and second level slow and fast processes. The two-layer L-96 model is used as a simple model for testing multiscale flow turbulence simulating the typical features of geophysical flows [41, 34].

(C) *The one-layer barotropic model with topography.* The one-layer barotropic system [42, 45, 68] is a basic geophysical model for the atmosphere or ocean with the essential geophysical effects of rotation, topography, and both deterministic and random forcing. It is defined based on the potential vorticity $q = \Delta \psi + h + \beta y$ with $\omega = \Delta \psi$ the relative vorticity, h the bottom topography, and β the rotational effect

$$
\begin{aligned}
\frac{\partial q}{\partial t} + \nabla^\perp \psi \cdot \nabla q + U \frac{\partial q}{\partial x} &= -\mathcal{D}(\Delta) \psi + \mathcal{F}(\mathbf{x}, t) + \Sigma(\mathbf{x}) \dot{W}(t), \\
\frac{dU}{dt} + \int \frac{\partial h}{\partial x} \psi(t) &= -\mathcal{D}_0 U + \mathcal{F}_0(t) + \Sigma_0 \dot{W}_0(t),
\end{aligned}
\tag{2.9d}
$$

This is one of the simplest model for geophysical turbulent while still maintains the skill to generate many interesting realistic features, for example, the change of strength and direction in the large-scale zonal jets [68, 70].

(D) *The two-layer quasi-geostrophic model with baroclinic instability.* The two-layer quasi-geostrophic model with baro-clinic instability [72, 77, 67] is one fully nonlinear fluid model defined in a two-dimensional periodic domain

$$
\frac{\partial q_\psi}{\partial t} + J(\psi, q_\psi) + J(\tau, q_\tau) + \beta \frac{\partial \psi}{\partial x} + U \frac{\partial}{\partial x} \Delta \tau = -\frac{\kappa}{2} \Delta (\psi - \tau) + \mathcal{F}_\psi(\mathbf{x}, t),
$$
$$
\frac{\partial q_\tau}{\partial t} + J(\psi, q_\tau) + J(\tau, q_\psi) + \beta \frac{\partial \tau}{\partial x} + U \frac{\partial}{\partial x} \left(\Delta \psi + k_d^2 \psi\right) = \frac{\kappa}{2} \Delta (\psi - \tau) + \mathcal{F}_\tau(\mathbf{x}, t).
$$

(2.9e)

It is capable in capturing the essential physics of the relevant internal variability including internal baroclinic instability. This model is useful for the investigation of climate change problems, such as the change of jet direction, the responses in the zonal mean jet strength, and the poleward heat transport in the atmosphere and ocean regimes [67].

We will use the above models next to illustrate the various features of linear and nonlinear statistical response theory and its applications to various problems.

Remark. The conditional Gaussian framework [41, 14] provides a rich group of models in understanding and predicting complex multiscale turbulent dynamics. The conditional Gaussian models take the general form

$$
d\mathbf{u_1} = [A_0(t, \mathbf{u_1}) + A_1(t, \mathbf{u_1}) \mathbf{u_2}] \, dt + \Sigma_1(t, \mathbf{u_1}) \, d\mathbf{W_1},
$$
$$
d\mathbf{u_2} = [B_0(t, \mathbf{u_1}) + B_1(t, \mathbf{u_1}) \mathbf{u_2}] \, dt + \Sigma_2(t, \mathbf{u_1}) \, d\mathbf{W_2}.
$$

(2.10)

Given the realization of the first state $\mathbf{u_1}(t), t < T$, the second state $\mathbf{u_2}$ becomes conditional Gaussian on the history of the state $\mathbf{u_1}$. Further, analytic formulas can be derived for the statistical mean and covariance matrix based on this conditional Gaussian structure [14]. Modified versions of the previous examples can be embedded into this conditional Gaussian structure (2.10) with suitably added noises.

2.3   Statistical linear response theory for turbulent systems

One important problem in the complex turbulence system (2.1) concerns about the accurate calibration of the model sensitivity to perturbations. Detecting the optimal response in the high dimensional phase space is crucial for the climate change science [27, 26, 23]. Direct solving the statistical equations (2.5) according to various climate change perturbations becomes expensive and mostly impractical. Statistical linear response theory [40, 46, 39, 81] provides an attractive alternative by expressing the statistical quantities subjected to small perturbations in term of statistics of an unperturbed state. Here we give a brief description for the theories and strategies in predicting model statistical responses.

2.3.1   Linear response theory for general perturbations

The statistical response theory and fluctuation-dissipation theorem (FDT) offer a convenient way to compute leading-order statistical approximation about model responses to various external perturbations [11, 40, 59, 50]. The general unperturbed system (2.1), $\delta \mathbf{F} = \mathbf{0}$, gives an invariant equilibrium measure $p_{\text{eq}}(\mathbf{u})$. The external forcing perturbation is written in separation with temporal and spatial variables,

$$
\delta \mathbf{F}(\mathbf{u}, t) = \mathbf{w}(\mathbf{u}) \, \delta f(t),
$$

where $\mathbf{w}(\mathbf{u})$ defines the spatial dependence and $f(t)$ defines the temporal variability of the forcing perturbations. The resulting perturbed probability density function p^δ due to the general forcing perturbation $\delta \mathbf{F}$ then can be asymptotically expanded according to the equilibrium and the correction to perturbation as

$$
p^\delta(\mathbf{u}, t) = p_{\text{eq}}(\mathbf{u}) + \delta p'(\mathbf{u}, t), \quad \int p_{\text{eq}}(\mathbf{u}) \, d\mathbf{u} = 1, \quad \int \delta p'(\mathbf{u}) \, d\mathbf{u} = 0.
$$

(2.11)

The statistical expectation of any functional $A(\mathbf{u})$ to the perturbation is formulated accordingly under the equilibrium mea-sure and leading-order correction, $\langle A(\mathbf{u}) \rangle = \langle A \rangle_{\text{eq}} + \delta \langle A \rangle(t) + O(\delta^2)$, using the measure asymptotic decomposition (2.11) with $\langle A \rangle_{\text{eq}} = \int A(\mathbf{u}) \, p_{\text{eq}}(\mathbf{u})$ the expectation of A according to equilibrium distribution p_{eq}, and $\delta \langle A \rangle = \int A(\mathbf{u}) \, \delta p'(\mathbf{u})$ according to the perturbation correction $\delta p'$. FDT gives the leading order prediction for the statistical response functional computed from the convolution with the linear response operator

$$
\langle A \rangle_{\text{eq}} = \int A(\mathbf{u}) \, p_{\text{eq}}(\mathbf{u}) \, d\mathbf{u}, \quad \delta \langle A \rangle(t) = \mathcal{R}_A * \delta f(t) = \int_0^t \mathcal{R}_A(t - s) \, \delta f(s) \, ds.
$$

(2.12)

The derivation of the above formula is concluded from separating the leading order dynamics of the Fokker-Planck equation for the perturbed probability function [40]. The pointed-bracket above denotes the statistical average under the solution p from the Fokker-Planck equation. $\mathcal{R}_A(t)$ is called the *linear response operator* corresponding to the functional A, which is calculated through correlation functions in the unperturbed statistical equilibrium only

$$\mathcal{R}_A(t) = \langle A[\mathbf{u}(t)] G[\mathbf{u}(0)] \rangle_{\mathrm{eq}}, \quad G(\mathbf{u}) = -p_{\mathrm{eq}}^{-1} \mathrm{div}_{\mathbf{u}}(\mathbf{w} p_{\mathrm{eq}}). \tag{2.13}$$

The noise term $\sigma \dot{W}$ is used to generate smooth equilibrium measure p_{eq} for computing the derivatives in the linear response operator $\mathcal{R}_A$. The FDT formula for statistical responses (2.12) is shown to have high skill for the mean response and some skill for the variance response for a wide variety of turbulent dynamical systems even with nonlinearity [46, 1, 51, 2, 37, 27]. In addition, rigorous theories [29, 43] have been provided for the validity of the linear response theory.

Still, the linear response operator $\mathcal{R}_A$ is difficult to calculate by directly using (2.13) for general systems considering the complicated and unaccessible equilibrium distribution p_{eq}. A variety of Gaussian approximations for p_{eq} and improved algorithms have been developed for computing the linear response operators [35, 40, 51, 43]. In many situations, it is found that a Gaussian PDF from the Gibbs invariant measure can offer a quite accurate characterization of the unperturbed distribution of the system (see explicit examples from Section 3 and 4). In this way, the *quasi-Gaussian* (qG) closure, $p_{\mathrm{eq}} \sim p_{\mathrm{eq}}^G$, provides a desirable approximation of the equilibrium measure. Then the linear response operator (2.13) can be computed directly from the autocorrection functions. The qG FDT has shown effective skill in predicting the statistical responses especially in the mean state, but less feasible for the higher-order moment predictions (see examples in [51, 46] and in Section 3).

2.3.2 Computing response operators with non-Gaussian statistics through kicked initial states

The difficulty in calculating the linear response operator using (2.13) is the expensive computational cost for general systems with non-Gaussian features in the equilibrium distribution p_{eq} in a high dimensional phase space. One strategy with higher accuracy (than using the quasi-Gaussian closure) to approximate the linear response operator avoiding direct evaluation of p_{eq} but still include important non-Gaussian statistics is through the *kicked response* by converting an unperturbed system to a perturbation $\delta \mathbf{u}$ of the initial state from the equilibrium measure. The idea is to set the initial distribution with the same equilibrium variance but a kick in the mean state so that

$$p\mid_{t=0} = p_{\mathrm{eq}}(\mathbf{u} + \delta \mathbf{u}) = p_{\mathrm{eq}} + \delta \mathbf{u} \cdot \nabla p_{\mathrm{eq}} + O(\delta^2). \tag{2.14}$$

One important advantage of adopting this kicked response strategy is that higher-order statistics due to nonlinear dynamics will not be ignored (compared with the other linearized strategy using only Gaussian statistics [46]). The validity of the kicked response strategy is guaranteed by the following proposition [40, 49] for calculating the linear response operator:

Proposition 2. *For δ small enough, the linear response operator $\mathcal{R}_A(t)$ can be calculated by solving the unperturbed system (2.1) with a perturbed initial state in (2.14). Then, the linear response operator can be achieved through the following formula by tracking the perturbed response in the unperturbed dynamics*

$$\delta \mathcal{R}_A(t) \equiv \delta \mathbf{u} \cdot \mathcal{R}_A = \int A(\mathbf{u}) \, \delta p' + O(\delta^2). \tag{2.15}$$

Above $\delta p'$ is the resulting leading order expansion of the transient probability density function from unperturbed dynamics using initial value perturbation.

From the formula (2.15), the response operator for the mean and variance can be achieved from the perturbation part of the probability density $\delta p'$. The proof of the above Proposition is a direct application of *Duhamel's principle* to the corresponding Fokker-Planck equation with the forcing perturbation [40]. The variability in the external forcing is transferred to the perturbation in initial values. More importantly, the kicked response formulation (2.15) with initial mean state perturbation (2.14) is independent of the specific perturbation forms. Thus the operator $\mathcal{R}_A$ describes the inherent dynamical mechanisms of the system.

Practical numerical strategies to compute the kicked response operators

The statistical kicked response strategy offers a practical method to compute the linear response operators especially for the unaccessible non-Gaussian equilibrium distributions. From the formula in (2.15), the response operators for the mean

and variance can be achieved from the perturbation part of the probability density $\delta p'$. In practice, $\delta p'$ can be either estimated from a direct Monte-Carlo simulation, or from a statistical model solution. Below we describe the numerical procedure to get this distribution function $\delta p'$ for general turbulent systems. See [40, 39] for a similar version of this algorithm.

- *Kicked response from direct model simulations*: A direct way to get the kicked PDF response $\delta p'$ is through a Monte-Carlo simulation of (2.1) using a large enough ensemble size to capture the leading statistical responses. The initial ensemble for the model simulation is sampled from the equilibrium distribution. For the kicked response to the mean, a constant small perturbation of the equilibrium mean state (for example, $\delta \mathbf{u} = 0.1 \bar{\mathbf{u}}_{\mathrm{eq}}$) is added to each initial ensemble members, while the initial variance of the ensemble is kept unchanged. The response distribution $\delta p'$ then is achieved by monitoring the decay of the ensemble mean back to equilibrium under unperturbed dynamics and uniformly perturbed initial value.

- *Kicked response from statistical models*: Another way to get the kicked response statistics is through the statistical model equations (2.5) to get the responses for the mean and variance. The initial mean state is taken from the equilibrium distribution with a perturbation (for example, $\delta \mathbf{u} = 0.1 \bar{\mathbf{u}}_{\mathrm{eq}}$). The initial value for the variance is taken the same as the equilibrium state value and kept unperturbed. Then starting from this initial mean and variance, the statistical model offers the kicked response solution to monitor the decay of the mean and variance back to equilibrium.

Compared with the qG closure using Gaussian statistics in the equilibrium measure, the kicked response gives a better quantification of the higher order statistics of the system since the nonlinear dynamics is better characterized. Therefore, the kicked response has more feasible prediction for systems with stronger nonlinearity and generates better results for higher order moments.

3 Statistically Accurate and Inaccurate Response Functionals and Reduced-Order Models for Nonlinear Responses

In this section, we display the skills in the statistical linear and nonlinear response theories under the framework of prototype models. With these simplified models, the basic properties of the statistical response functionals with accurate and inaccurate prediction skills can be characterized in a precise way. More realistic applications for the two-dimensional barotropic turbulence is then carried out next in Section 4.

Low-frequency stochastic models offer an attractive first testing framework for understanding the basic properties in the statistical response theory. A one-dimensional exactly solvable model with additive and multiplicative noises

$$du = \left(f + au + bu^2 - cu^3\right) dt + (A - Bu)\, dW_1 + \sigma dW_2, \tag{3.1}$$

has been first used to show the typical features in FDT [46, 48]. This model provides the simplest tool in the investigation of low-frequency variability in the long time atmospheric or climate sensitivity studies. Especially, explicit unperturbed distribution solution can be found for the model (3.1) by directly solving the associated Fokker-Planck equation. The explicit formulation of the stochastic model enables us to calculate the response operators based on different response functionals $A(\mathbf{u})$ using Gaussian (and conditional Gaussian) statistics. Another desirable property of the stochastic low-frequency model (3.1) is that it generates a wide range of different statistical regimes from uni-modal near-Gaussian PDFs to skewed non-Gaussian distributions by changing the parameter values. This is also similar to the features in the general atmospheric circulation models.

Next, we compare the accuracy in the Gaussian and quasi-Gaussian response theory with kicked initial state using nonlinear prototype models without explicit solvable expressions.

3.1 Empirical information theory for measuring imperfect model errors

In most practical cases, the exact equilibrium distribution p_{eq} is unavailable due to the complex nonlinear coupling between scales. Therefore, imperfect approximation and calibration of the model invariant distributions with error is the first problem to consider. The information-theoretic framework [31, 40] provides an unbiased metric to quantify the imperfect model sensitivity by building the least biased probability measure consistent with the true system. Information theory is often used in statistical science for imperfect model selection [9]. A natural way to measure the lack of information

in one probability density with approximation, p^M, compared with the true probability density, p, is through the *relative entropy* (or *information distance*) [33, 40], given by

$$\mathcal{P}\left(p, p^M\right) = \int p \log \frac{p}{p^M}. \tag{3.2}$$

The relative entropy guarantees the following two crucial features to serve as a metric: (i) $\mathcal{P}\left(p, p^M\right) \geq 0$, and the equality holds if and only if $p = p^M$; (ii) it is invariant under any invertible change of variables. Despite the lack of symmetry in its arguments (that is, $\mathcal{P}\left(p_1, p_2\right) \neq \mathcal{P}\left(p_2, p_1\right)$ in general), the relative entropy, $\mathcal{P}\left(p, p^M\right)$ provides an attractive framework for assessing model error and sensitivity like a probabilistic metric.

Usually, the first entry p is used to denote the probability distribution of the perfect model, which is unknown. Nevertheless, we can construct an estimate distribution p_L of the perfect model using first L measurements of the true system. Consider the imperfect model prediction with its associated probability density p_L^M, the definition of relative entropy (3.2) facilitates the practical calculation [32, 49, 50, 45, 47]

$$\mathcal{P}\left(p, p^M\right) = \mathcal{P}\left(p, p_L\right) + \mathcal{P}\left(p_L, p_L^M\right).$$

The entropy difference $\mathcal{P}\left(p, p_L\right)$ precisely measures an intrinsic error from L measurements of the perfect system, and this offers a simple example of an information barrier for any imperfect model based on L measurements for calibration. The most practical setup for utilizing the framework of empirical information theory arises when only the Gaussian statistics (that is, the first two moments) of the distributions are computed. With the measurements $L = 2$ representing the first two moments, a Gaussian approximation can be used to estimate the information error $\mathcal{P}\left(p_L, p_L^M\right)$ considering only the first $L = 2$ statistical measurements. By only comparing the first two moments of the density functions, we get the following fact [40]:

Proposition 3. *If the probability density functions* p_L, p_L^M *contain only the first two moments, that is,* $p \sim \mathcal{N}\left(\bar{\mathbf{u}}, R\right)$ *and* $p^M \sim \mathcal{N}\left(\bar{\mathbf{u}}_M, R_M\right)$, *the relative entropy in (3.2) has the explicit formula*

$$\mathcal{P}\left(p_L, p_L^M\right) = \frac{1}{2}\left(\bar{\mathbf{u}} - \bar{\mathbf{u}}_M\right)^T R_M^{-1}\left(\bar{\mathbf{u}} - \bar{\mathbf{u}}_M\right) + \frac{1}{2}\left(\operatorname{tr}\left(RR_M^{-1}\right) - N - \log\det\left(RR_M^{-1}\right)\right). \tag{3.3}$$

The first term on the right hand side of (3.3) is called the *signal*, reflecting the model error in the mean and weighted by the inverse of the model variance R_M; whereas the second term is the *dispersion,* including only the model error covariance ratio RR_M^{-1}, measuring the differences in the covariance matrices.

For measuring the model sensitivity in the linear response statistics (2.11), we have $p_\delta = p_{\text{eq}} + \delta p$ for the true model, and $p_\delta^M = p_{\text{eq}}^M + \delta p^M$ for the imperfect model approximation. In the case with equilibrium consistency, that is, the imperfect model gives the exact unperturbed invariant measure $\mathcal{P}\left(p_{\text{eq}}, p_{\text{eq}}^M\right) = 0$, the relative entropy in (3.3) between perturbed model density p_δ^M and the true perturbed density p_δ with small perturbation δ can be expanded in the leading order terms as

$$\mathcal{P}\left(p_\delta, p_\delta^M\right) = \mathcal{P}\left(p_{L,\delta}, p_\delta\right) + \frac{1}{2}\int p_{L,\text{eq}}^{-1}\left(\delta p - \delta p^M\right)^2 + O\left(\delta^3\right). \tag{3.4}$$

Above, the first part $\mathcal{P}\left(p_{L,\delta}, p_\delta\right)$ is the intrinsic error from only first L measurements of the system. The second quadratic term is called the Fisher information metric [80, 43, 41]. Under Gaussian statistical closure in the two distributions $p = p_G$ and $p^M = p_G^M$, the Fisher information can be expanded componentwise in the perturbation of the mean and variance as

$$\underbrace{\frac{1}{2}\sum_k \left(\delta\bar{u}_k - \delta\bar{u}_{M,k}\right) r_k^{-1}\left(\delta\bar{u}_k - \delta\bar{u}_{M,k}\right)}_{\text{signal}} + \underbrace{\frac{1}{4}\sum_k r_k^{-2}\left(\delta r_k - \delta r_{M,k}\right)^2}_{\text{dispersion}}. \tag{3.5}$$

Above, r_k is the equilibrium variance in k-th component, and $\delta\bar{u}_k$ and δr_k are the linear response operators for the mean and variance in k-th component. The information theory plays an important role in quantifying model error, model sensitivity and information barrier. Next, we illustrate the calibration of model error in the response theories using explicit examples with multiscale structures.

3.2 Linear response functionals using the two-layer Lorenz '96 Model

We first use the inviscid two-layer L-96 model introduced in (2.9c) to display the validity of linear response theory for systems with multiscale structures

$$\frac{du_j}{dt} = (u_{j+1} - u_{j-2}) u_{j-1} - \lambda \sum_k v_{j,k} + F_j,$$

$$\frac{dv_{j,k}}{dt} = \frac{1}{\epsilon} v_{j,k+1} (v_{j,k-1} - v_{j,k+2}) + \lambda u_j.$$

The two-layer L-96 model is characterized by two sets of slow-fast processes $(u_j, v_{j,k})$. The variable u_j with $1 \leq j \leq J$ represents the slow varying climate, while $v_{j,k}$ with $1 \leq k \leq K$ according to each slow process u_j gives the set of fast varying weather with the total size JK. The parameter λ defines the coupling coefficient between the two scales u_j and $v_{j,k}$; $\epsilon > 0$ defines the time scale separation between the two processes. In this test case, we assume zero external forcing $F_j \equiv 0$ in the unperturbed equilibrium. More discussion about detailed properties and physical interpretations of the two-layer L96 can be found in [34, 14].

3.2.1 Explicit linear response operators from the Gibbs invariant measure

The total energy $E(u, v)$ combining both slow and fast variables of the two-layer L-96 model is conserved for the inviscid flow without any damping and forcing effects. This implies the classical Gibbs invariant measure with zero mean and equipartition of energy at each grid defined as the climate

$$p_{eq}(u, v) = C^{-1} \exp\left(-\frac{1}{2\sigma_{eq}^2} E(u, v)\right), \quad E(u, v) = \sum_{j=1}^{J} \left(u_j^2 + \sum_{k=1}^{K} v_{j,k}^2\right), \tag{3.6}$$

where σ_{eq}^2 gives the homogeneous variance at each grid [40, 42]. Therefore, the linear response operator $\mathcal{R}_A$ in (2.13) can be computed directly using the explicit formulation of p_{eq} from the Gibbs invariant measure. To test the accuracy in the linear responses with perturbations in large and small scale variables, we consider homogeneous perturbations added to the large-scale state $F_j = \delta F$. This forcing perturbation can be viewed at the climate change effect introduced to the slow-varying climate. Still both large and small scale variables will be affected by this large scale climate changing forcing. As a direct conclusion using the statistical energy principle in (2.8), the total statistical energy in the system $\langle E \rangle = \int E(u, v) p(u, v) \, du \, dv$ about the perturbed probability distribution p can be found only dependent on the forced response mean state

$$\frac{d\langle E \rangle}{dt} = \sum_j \delta F_j \cdot \bar{u}_j, \quad \langle E \rangle = \sum_{j=1}^{J} \left(\langle u_j^2 \rangle + \sum_{k=1}^{K} \langle v_{j,k}^2 \rangle\right). \tag{3.7}$$

This implies that the total statistical energy of the system is determined only by the large-scale homogeneous mean state $\bar{u}_j \equiv \bar{u}$. Notice that the statistical energy $\langle u_j^2 \rangle, \langle v_{j,k}^2 \rangle$ contain the variabilities in both energy in the mean, $\bar{u}^2$, and the variance, $\overline{u'^2}$. The total variance in the inviscid system will keep increasing due to the constant forcing effect $\delta F \cdot \bar{u}$ with a final saturated mean state $\bar{u}$.

Next, we compute the detailed statistical responses for the mean and variance according to the homogeneous large scale perturbation $F_j = \delta F$. By directly applying the formula (2.13), the corresponding operators G_u using the quasi-Gaussian (qG) Gibbs measure (3.6) can be computed explicitly as

$$G_u = -\frac{\sum_j \partial_{u_j} p_{eq}}{p_{eq}} = \sum_{j=1}^{J} \frac{u_j}{\sigma_{eq}^2}.$$

Again, due to the homogeneous statistics in the unperturbed equilibrium measure of the model, the cross-covariances between different grids vanish in the final state, $\langle u_i^s(t) u_j(0) \rangle_{eq} = 0$ for $i \neq j$. The explicit formulas for the qG response operators for the mean and variance of the large and small scale homogeneous variables can be computed as

$$\text{large scale response} : \mathcal{R}_u = \frac{\sigma_{eq}^{-1}}{J} \sum_j \langle u_j(t) u_j(0) \rangle_{eq}, \quad \mathcal{R}_{u^2} = \frac{\sigma_{eq}^{-1}}{J} \sum_j \langle u_j^2(t) u_j(0) \rangle_{eq};$$

$$\text{small scale response} : \mathcal{R}_v = \frac{\sigma_{eq}^{-1}}{JK} \sum_{j,k} \langle v_{j,k}(t) u_j(0) \rangle_{eq}, \quad \mathcal{R}_{v^2} = \frac{\sigma_{eq}^{-1}}{JK} \sum_{j,k} \langle v_{j,k}^2(t) u_{j,k}(0) \rangle_{eq}. \tag{3.8}$$
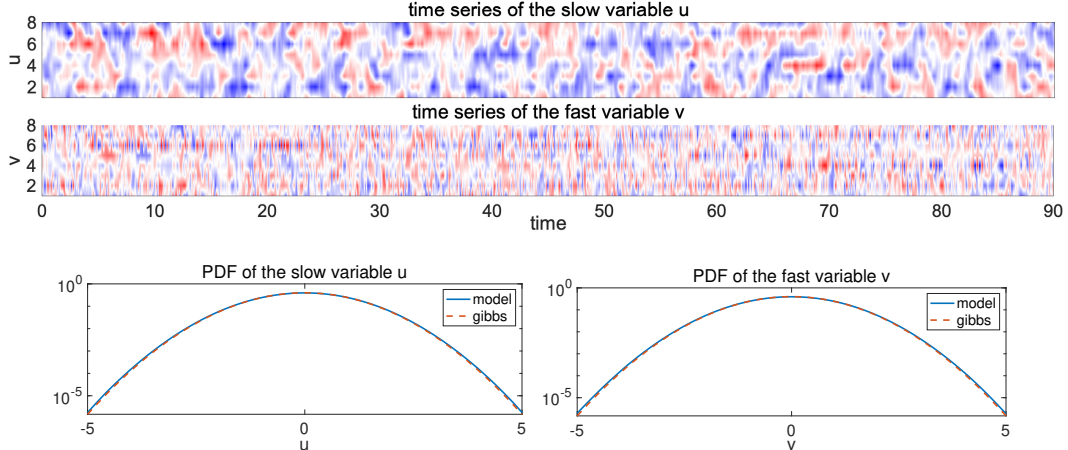
Figure 3.1: Illustration of the multiscale two-layer L-96 model solution and equilibrium homogeneous statistics with $J = K = 8$ and $\lambda = 1, \epsilon = 0.1, F = 0$. Upper row: space-time diagram of the slow and fast state solutions (u, v) (the fast variable $v_{i,j}$ is evaluated at one fixed value $j = 1$); second row: marginal PDFs of the equilibrium slow and fast variables compared with the invariant Gibbs measure.

Above, $\mathcal{R}_u$ is the response operator for the homogeneous large-scale mean $\langle u_j \rangle \equiv \bar{u}$; and $\mathcal{R}_{u^2}$ is the response operator for the homogeneous large-scale variance $\left\langle (u_j - \bar{u})^2 \right\rangle \equiv r$. Similar case applies for the small scale variables $v_{j,k}$. The linear response operators are computed under the statistical average about the equilibrium measure. From (3.8) using the Gaussian equilibrium distribution (3.6), the response function from the large scale perturbation is the autocorrelation functions, while the response function for the small scales comes from the lagged cross-correlation between the small-large scale states at the some grid, $u_j, v_{j,k}$.

Finally, using the response operators (3.8), the statistical responses in mean and variance subject to the constant in time large scale perturbation δF can be computed directly from the convolution formula (2.12) as an integration of the linear response operators

$$\delta \bar{u}(t) = \delta F \int_0^t \mathcal{R}_u(\tau) \, d\tau, \quad \delta r_u(t) = \delta F \int_0^t \mathcal{R}_{u^2}(\tau) \, d\tau.$$

Above, $\mathcal{R}_{\bar{u}}(t)$ and $\mathcal{R}_r(t)$ are the response operators corresponding to the forcing perturbation. This gives the FDT prediction of the mean and variance responses in both large and small scales. Due to the homogeneous statistics in the equilibrium measure as well as the forcing perturbation forms, the statistical response stays uniform at each grid point. Finally the accuracy of the statistical predictions can be measured under the information metric constraint on the first two moments using the formula (3.5).

3.2.2 Numerical tests for the accurate and inaccurate linear response predictions

In the numerical tests, we take the model dimensions $J = 8$ and $K = 8$ (that is, with 8 variables in the slow state u and in total 64 variable in the fast state v). The value of the coupling parameter is taken as $\lambda = 1$ and the time-scale separation is set as $\epsilon = 0.1$. Zero external forcing $F \equiv 0$ is assumed for the unperturbed equilibrium state of the system. Similar reference parameters are adopted in [46]. Figure 3.1 offers the direct simulation result for the unperturbed two-layer L-96 model PDFs. Both the slow and fast variables (u, v) agree with the Gaussian distribution predicted in the Gibbs invariant measure with unit equilibrium variance $\sigma_{\text{eq}} = 1$. The time-series show a more rapid time scale in the fast variable v than the slow variable u.

Then we compare the accuracy using the quasi-Gaussian (qG) FDT and kicked response FDT in this two-layer L-96 system and the errors are measured in the information metrics. Particularly, we test the skills in the prediction of large and small scale responses in their mean and variance with only homogeneous large scale perturbation $F_j = \delta F$. First, Figure 3.2 displays the linear response operators for the mean and variance responses in large scale u and small scale v. Results from the two strategies using the kicked response and the qG closure are compared. For the response in the mean state, the two methods offers similar approximation for the linear response operator. This implies comparable skill in predicting mean responses using both approximations. For the response in the variance, however, the kicked response
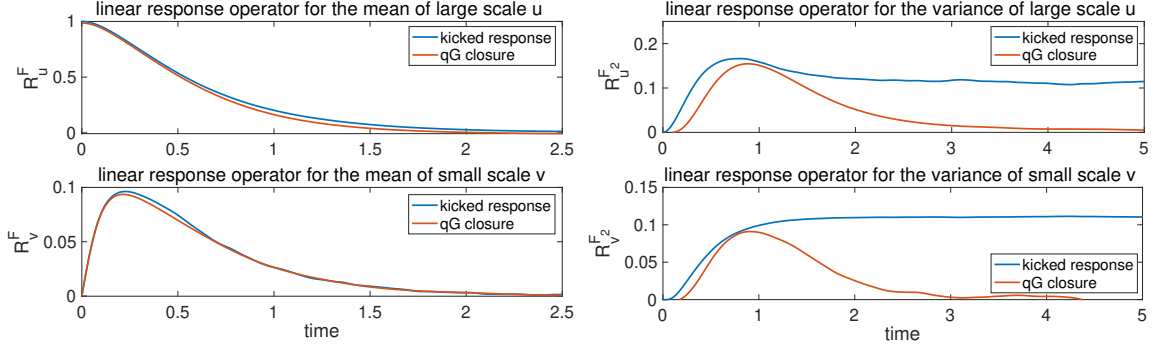
Figure 3.2: Linear response operators for the large and small scale mean (left) and variance (right) responses. The operators computed from the kicked response strategy is compared with the qG closure using the Gaussian Gibbs invariant measure.

generates non-zero response in the long time limit, while the qG closure just captures the transient changes in variance and decays to zero at the long time limit from the autocorrelation functions. This difference shows the less accuracy in the qG approximation for predicting second order moments. Clearly from the total statistical energy equation (3.7), the variance should keep increasing in the inviscid model with a non-zero mean generated.

At last, we show the FDT prediction skills using the linear response operators for the statistical response in mean and variance. Figure 3.3 plots the statistical response predictions in mean and variance using both kicked FDT and qG FDT approximations. Two different homogeneous constant forcing perturbation amplitudes $\delta F = 1$ and $\delta F = 0.5$ are also compared for testing the accuracy with different nonlinearity. The accuracy of the predictions is calibrated using the relative entropy metric (3.5) as a balanced combination of the error in the mean (signal error) and the error in the variance (dispersion error). First in the prediction for the mean responses, both kicked response and qG closure do a good job especially in capturing the starting transient state responses. The prediction for the large scale u is also easier with higher accuracy than that of the small scale v. With a large perturbation amplitude $\delta F = 1$, stronger nonlinear effect gradually takes over. The statistical response theory fails to capture the long time drop in the mean, especially for the small scale variables v. In signal error shows the high skills in both methods.

Second in the variance response, the inviscid model with constant forcing leads to a persistent growth in the variance. The qG FDT fails in this case to predict the long time variance response and cannot capture the persistent growth. The kicked FDT offers a better prediction for the increasing trend in the variance in both large and small scales. Still, the response theory lacks the skill to get the exact rate of increasing with accuracy in the second moments. The dispersion error offers a more precise calibration of the errors in the two methods. It can be seen that the qG closure gives a better estimation in the short time transient state for the variance response in both small and large scales. At the long time limit, the kicked response becomes more skilled at getting the growing trend in the variance, while the qG closure simply goes to zero leading to larger errors. In general, the large scale variability is easier to capture than the rapidly changing small scale responses.

3.3 Strategies in predicting nonlinear responses using reduced-order statistical models

The previous example with the multi-scale L-96 system displays explicitly the extent of skills of the linear response theory to predict the statistical responses. Using FDT with the linear response operators, the short-time transient changes with small amplitude perturbations can be captured with desirable accuracy in the first-order moment. On the other hand, when it comes to regimes with strong nonlinearity and higher order moments (including the variance), the linear response theory considering only the leading order expansion becomes less sufficient in getting the statistical variability with accuracy.

Therefore, more detailed calibration for the turbulent system becomes a necessary when we want to capture the nonlinear responses in a wider range of perturbations. Here we present the basic ideas in the statistically accurate reduced-order models as a more effective strategy in predicting the nonlinear responses [39, 45]. Before preceding to the applications in a more realistic high-dimensional turbulent system in Section 4, the basic ideas in developing the reduced-order statistical model framework are offered using the triad model (2.9a) as a special case of the general formulation (2.1)

13
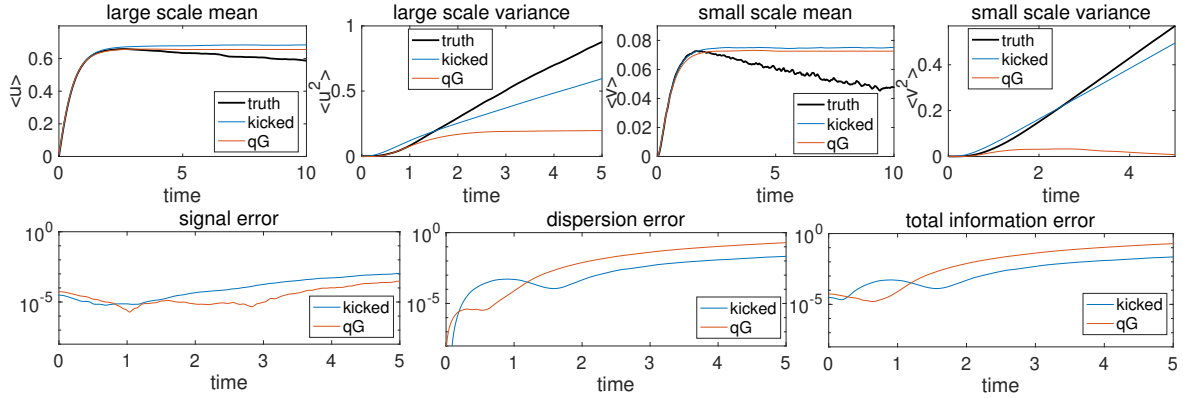
(a) responses with forcing perturbation $\delta F = 1$
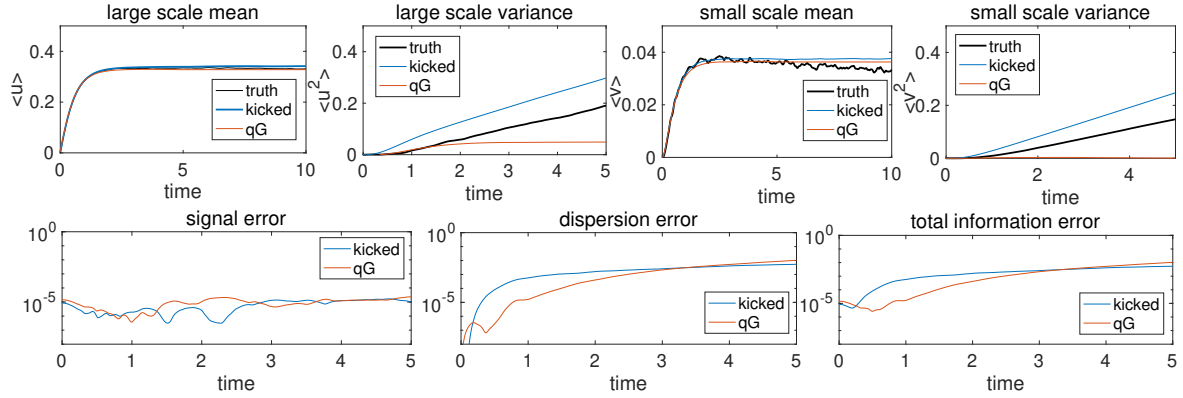
(b) responses with forcing perturbation $\delta F = 0.5$

Figure 3.3: Responses in mean and variance in large and small scale variables using two constant forcing perturbations $\delta F = 1$ and $\delta F = 0.5$. The predictions using kicked FDT and qG FDT are compared with the truth from direct Monte-Carlo simulations. The accuracy of the prediction is calibrated under the information metrics for the signal (mean), dispersion (variance), and total information distance.

by letting

$$L = \begin{bmatrix} 0 & -L_3 & L_2 \\ L_3 & 0 & -L_1 \\ -L_2 & L_1 & 0 \end{bmatrix}, \ D = \begin{bmatrix} -d_1 & & \\ & -d_2 & \\ & & -d_3 \end{bmatrix}, \ \mathbf{F} = \begin{bmatrix} F_1 \\ F_2 \\ F_3 \end{bmatrix}, \ \boldsymbol{\sigma} = \begin{bmatrix} \sigma_1 & & \\ & \sigma_2 & \\ & & \sigma_3 \end{bmatrix}.$$

3.3.1 Ideas in calibrating and predicting the nonlinear statistical responses

In general, the reduced-order statistical modeling strategy is carried out in three stages: i) imperfect model selection according to the complexity of the problem; ii) model calibration in a training phase using equilibrium data; and iii) model prediction with the optimized model parameters for various responses to external perturbation. Compared with the linear response theory, the nonlinear dynamics are modeled explicitly in the reduced-order models. Specifically in the reduced-order models to be developed here, we will consider additional damping and random noise corrections for the unresolved higher-order statistics. The equilibrium invariant measure and ergodic theory [56, 74] can help determine the existence of a smooth invariant measure for the reduced-order model. The linear response operators from the unperturbed equilibrium measure in turn help improve the nonlinear response prediction through the model calibration.

Generally the statistical model for the leading two moments can be derived from the full statistical model (2.5) with a large scale projection

$$\frac{d\bar{\mathbf{u}}_M}{dt} = (L + D)\,\bar{\mathbf{u}}_M + B\,(\bar{\mathbf{u}}_M, \bar{\mathbf{u}}_M) + R_{M,ij} B\,(\mathbf{e}_i, \mathbf{e}_j) + \mathbf{F},$$
$$\frac{dR_M}{dt} = L_v\,(\bar{\mathbf{u}}_M)\,R_M + R_M L_v^*\,(\bar{\mathbf{u}}_M) + Q_F^M + Q_\sigma, \tag{3.9}$$

where $\bar{\mathbf{u}}_M = \mathcal{P}_M \bar{\mathbf{u}}$ is the model approximated mean, and R_M is the reduced order covariance matrix about the fluctuation state variable $\mathbf{u}'$. The most expensive but crucial part comes from the nonlinear flux term Q_F where important third-order moments are included representing the nonlinear interactions between different modes. A hierarchical statistical model reductions are constructed with a judicious estimation about this nonlinear interaction term

$$Q_F^M = Q_F^- + Q_F^+ = -D_M\,(R)\,R_M - R_M D_M^*\,(R) + \Sigma_M\,(R), \tag{3.10}$$

through a series of constructions with increasing complexity [53, 68, 67, 39]. The negative-definite $Q_F^- = -D_{M,k}\,(R)\,R_M - R_M D_{M,k}^*\,(R)$ represents the additional damping effect to stabilize the unstable modes with positive Lyapunov coefficients, while $Q_F^+ = \Sigma_{M,k}\,(R)$ is the positive-definite additional noise to compensate for the overdamped modes. In the model parameters, (D_M, Σ_M) replaces the original nonlinear unstable and stable effects from the original dynamics. The approximation error in the imperfect model is calibrated through the linear response theory. Two crucial components in the construction of (3.10) are: first, equilibrium statistical fidelity using the unperturbed equilibrium statistics $\left(Q_{F,\mathrm{eq}}^+, Q_{F,\mathrm{eq}}^-\right)$, which can be computed easily from the steady state equations (2.5) using lower order statistics; and second, the improvement of model sensitivity using the total statistical energy E by solving the additional scalar equation (2.8). The detailed discussion for the step-by-step construction of the reduced model parameters can be found in [45, 39].

Reduced model calibration using statistical response theory

It is important to realize that equilibrium fidelity is a necessary but not sufficient condition for model predictions [45, 50, 39]. Accurate forecast of the nonlinear forced responses requires the correct representation of model's 'memory' to its previous history. In the linear response theory (2.12), the linear response operator $\mathcal{R}_A$ provides a unified way to quantify the model sensitivity in the imperfect models. The imperfect models can maintain high performance for various kinds of external perturbations if they are able to recover the response operator with desirable accuracy. Thus the optimal model parameter can be selected through minimizing the information distance in the linear response operators in (3.5) between the imperfect closure models and the truth.

The model calibration procedure is usually carried out in a training phase before the prediction, so that the optimal imperfect model parameters can be achieved through a careful calibration about the true higher-order statistics. The ideal way is to find a unified systematic strategy where various external perturbations can be predicted from the same set of optimal parameters through this training phase. To achieve this, various statistical theories and numerical strategies need to be blended together in a judicious fashion. Most importantly, we need to consider the linear statistical response theory to calibrate the model responses in mean and variances [40, 43, 29]; and use empirical information theory [49, 50, 42] to get a balanced measure for the error in the leading order moments. In the final model prediction stage, the optimal imperfect model parameters are applied for the forecast of various model responses to perturbations.
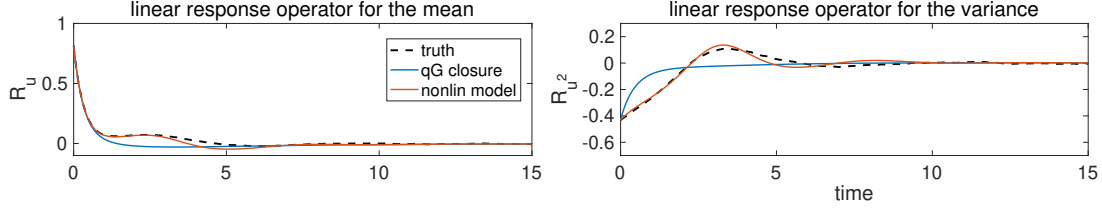
Figure 3.4: Linear response operators for the mean and variance in the triad model. The truth from the kicked response (dashed black) is compared with approximation from the nonlinear statistical model (red) using optimal parameters and the quasi-Gaussian closure approximation (blue).

Next, we illustrate the skills of the reduced statistical model in capturing nonlinear statistical sensitivity using the simple triad model.

3.3.2   Predicting statistical responses in the triad system

The triad system (2.9a) where three modes interact through the energy-conserving coupling term form the building block for more complex turbulent flows. It provides a simple first test case to show the model reduction strategy in the first stage. This model mimics the nonlinear interaction of two Rossby waves forced by baroclinic processes with a zonal jet forced by a polar temperature gradient. By changing the model parameters, a wide range of statistics are generated from near-Gaussian to highly non-Gaussian PDFs. The typical performance using the statistical response operators for effective model reduction is discussed in depth in [39, 45].

Model calibration in the training stage

In the tests using the triad model, we pick the dual energy cascade regime where $d_1 = 1, d_2 = 2, d_3 = 2$, $\sigma_1^2 = 10, \sigma_2^2 = 0.01, \sigma_3^2 = 0.01$, and the energy-conserving nonlinear coupling coefficients $B_1 = 2, B_2 = B_3 = -1$ and the skew-symmetric interactions as $L_1 = 0.09, L_2 = 0.06, L_3 = -0.03$. In this parameter regime, energy cascades in both direction between the 'large scale' u_1 and 'small scales' u_2 and u_3, leading to a highly non-Gaussian equilibrium distribution (see [39] for the PDFs). The linear response operators for the mean and variance are used to tune the parameters in the nonlinear statistical model. Through the discussions about linear response theory in Section 2.3, the true response operator is approximated from the kicked response strategy. The optimal parameter values in the reduced statistical model (3.9) are achieved through minimizing the distance in the model linear response operators under the information metric. Figure 3.4 shows the linear response operators in mean and variance due to deterministic and stochastic perturbations. Using the optimal parameters, the nonlinear reduced model gives good recovery of the true linear response effect in both mean and variance. Similar with the previous tests, the qG closure lacks the skill in capturing the sensitivity in the variance response when the non-Gaussian statistics of the system become important.

Model prediction to perturbations

In showing the reduced model skill in capturing the nonlinear responses to forcing perturbations, periodic perturbation is added to both the deterministic and random components of the external forcing in the triad system. The numerical results are summarized in Figure 3.5. The nonlinear reduced order model prediction is compared with the linear response theory results using the qG closure. Consistent with the previous discussions in Section 3.2, the qG FDT maintains the skill in capturing the responses in the mean with agreeable accuracy. From the signal errors for the mean, the qG FDT is just a little worse than the reduced model results with agreeable accuracy. On the other hand, the linear response theory fails to capture the responses in the higher order variance accurately especially for the two fast processes. In contrast, the reduced statistical model gives accurate predictions in the statistical responses in both mean and variance in slow and fast variables. The improvement is obvious from comparison of the information errors.
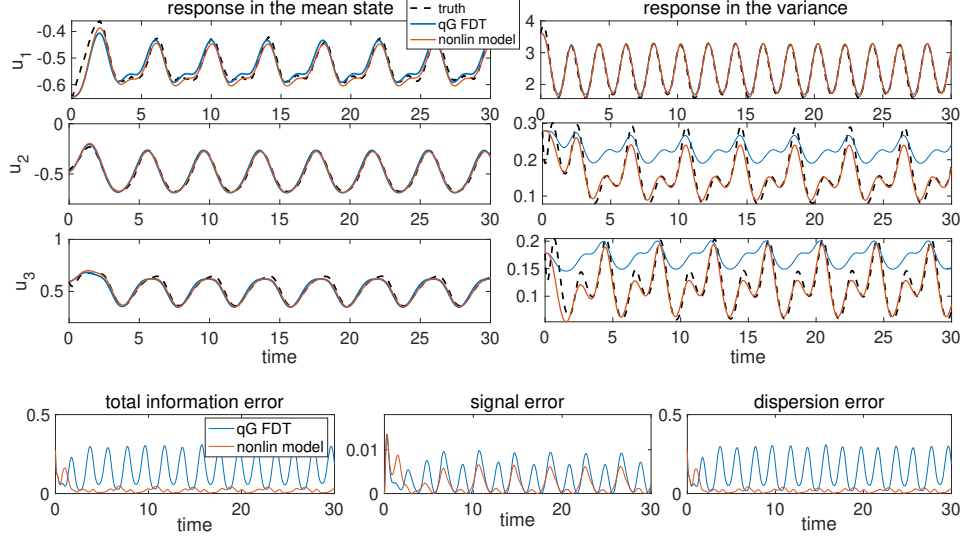
Figure 3.5: Prediction of nonlinear statistical response in mean and variance in the triad model subject to periodic perturbation. The prediction using the nonlinear reduced model is compared with the qG linear response prediction. The truth is achieved from direct Monte-Carlo simulations.

4 Linear and Nonlinear Statistical Responses for Barotropic Flows with Topography

To extend the validity of the statistical response theory to problems in a more realistic geophysical setting, the topographic barotropic system [42, 68] serves as a stringent model with higher complexity. This model offers a detailed interacting mechanism between small-scale eddies and a dynamically evolving large-scale flow. Here we show that a reduced-order model in only 3-dimensional resolved subspace is capable of capturing the principal statistics in first and second moments with desirable accuracy and efficiency. Despite the unavoidable model errors, the low-order approximation model displays uniform ability in predicting strong nonlinear responses to various external perturbations through the statistical response framework. In addition, a rigorous statistical saturation bound can be found for constraining the statistical range which the model responses can change inside.

4.1 Topographic barotropic system with interacting zonal mean flows

A basic group of simple models that incorporate the essential structures in geostrophic turbulence is the ideal barotropic quasi-geostrophic equations with a large-scale zonal mean flow and topographic effect [10, 42, 65]. The governing equations for the topographic barotropic turbulence are formulated on a rotational β-plane with doubly periodic boundary condition on $[-\pi, \pi] \times [-\pi, \pi]$ as

$$\frac{\partial \omega}{\partial t} + \nabla^\perp \psi \cdot \nabla q + \beta \frac{\partial \psi}{\partial x} + U \frac{\partial q}{\partial x} = -\mathcal{D}(\Delta)\psi + \mathcal{F}(\mathbf{x}, t) + \Sigma(\mathbf{x})\dot{W}(t),$$

$$\frac{dU}{dt} + \int \frac{\partial h}{\partial x} \psi(t) = -\mathcal{D}_0 U + \mathcal{F}_0(t) + \Sigma_0 \dot{W}_0(t),$$

(4.1)

where $q = \omega + h$, $\omega = \Delta\psi$ are the potential vorticity and relative vorticity respectively; and ψ is the stream function; h is the topographic structure while q is advected by the velocity field, $\mathbf{v} = \nabla^\perp \psi \equiv (-\partial_y \psi, \partial_x \psi)$. The interacting topographic Rossby waves from small-scale vortices ω are coupled with a large scale zonal jet U through the topography h. General dissipation and deterministic and random forcing are added on both small and large scale states. The system (4.1) creates anisotropic flows with a strong meandering zonal jets qualitative resembling to those observed in midlatitude ocean/atmosphere and laboratory experiments on topographic blocking [79, 28].

The dynamical equations without forcing and dissipation conserve both the *kinetic energy E* and the *large-scale*

enstrophy W [42] defined as

$$E = \frac{1}{2}U^2 + \frac{1}{2}\int |\nabla\psi|^2, \quad W = \beta U + \frac{1}{2}\int q^2. \tag{4.2}$$

It shows that these quadratic invariants have a crucial role in prediction of nonlinear responses and the analysis of nonlinear stability theory [45, 10]. In the application to the statistical response theory, next we introduce the statistical characterization of the system in unperturbed equilibrium and perturbed states.

4.1.1 Equilibrium invariant measure for the unperturbed barotropic flow

In geophysical turbulence, it is reasonable to assume that the unperturbed long-time averaged state (that is, the climate) is known with accuracy [10, 42]. The central quantity of interest becomes the fluctuations about the climate state. A special form of the exact steady state solution with linear dependence between the stream function and potential vorticity is often assumed [42] as

$$Q_{\text{eq}} = \Delta\Psi_{\text{eq}} + h = \mu\Psi_{\text{eq}}, \quad U_{\text{eq}} = -\beta/\mu. \tag{4.3}$$

The steady state is defined by the parameter μ. The linearly dependent solution is also predicted as the most probable state from the maximum entropy principle where the entropy is maximized with constant energy with μ as the Lagrangian multiplier [42, 10]. We focus on the responses in statistics in the fluctuation components $\tilde{\psi}_\mu = \psi - \Psi_{\text{eq}}(\mu)$ and $\tilde{U}_\mu = U - U_{\text{eq}}(\mu)$ about the climate state. For simplification in representations, the 'tildes' for the fluctuations are neglected in the rest part of this section.

The general statistical theories (2.8) can be applied to the fluctuation states of the barotropic flow. The system is projected on a finite dimensional subspace through a Galerkin truncation of high wavenumber N under standard Fourier basis $\mathbf{e_k} = \exp(i\mathbf{k}\cdot\mathbf{x})$

$$\omega_N = \sum_{1\leq k\leq N}\hat{\omega}_\mathbf{k}e^{i\mathbf{k}\cdot\mathbf{x}}, \quad \psi_N = \sum_{1\leq k\leq N}\hat{\psi}_\mathbf{k}e^{i\mathbf{k}\cdot\mathbf{x}} = -\sum_{1\leq k\leq N}k^{-2}\hat{\omega}_\mathbf{k}e^{i\mathbf{k}\cdot\mathbf{x}},$$

where ψ_N is the truncated stream function, $\omega_N = \nabla^2\psi_N$ is the truncated small-scale relative vorticity, and $k = |\mathbf{k}|$ is the wavenumber amplitude. A Gibbs invariant measure thus can be constructed [68] as a Gaussian distribution based on the conserved quantities (4.2)

$$p_{\text{eq}}(U,\omega) = C_{\text{eq}}^{-1}\exp\left[-\frac{\mu}{2}\sigma_{\text{eq}}^{-2}U^2 - \frac{1}{2}\sigma_{\text{eq}}^{-2}\sum_k\left(1+\mu k^{-2}\right)|\omega_\mathbf{k}|^2\right], \quad \sigma_{\text{eq}}^2 = \frac{\sigma^2}{2d}. \tag{4.4}$$

Notice that above (U,ω) are the fluctuation components centered at the climate state $(\bar{U}_{\text{eq}}, \bar{\omega}_{\text{eq}})$. This Gibbs measure is given by the conserved energy and enstrophy constraints [42]. One obvious drawback in the above invariant measure (4.4) is that it becomes unrealizable when $\mu < 0$. We will address this issue later in Section 4.4.

In fact, It can be confirmed that $p_{\text{eq}}(U,\omega)$ with the realizable parameter $\mu > 0$ is indeed the invariant measure in equilibrium through direct substitution into Fokker-Planck equation [45]. Proper damping and forcing operators are required on the right hands of (4.1). The admissible damping and forcing consistent with the Gaussian invariant measure (4.4) can be constructed [68] as

$$-\mathcal{D}_k\psi + \Sigma_k\dot{W}_k = -d\lambda_k\omega_k + \sigma_k\lambda_k^{1/2}\dot{W}_k, \quad \mathcal{F}_k = \delta F_k \equiv 0, \tag{4.5}$$

with $k = 0$ for the large scale forcing for U and $k \geq 1$ the vortical modes. Specific amount of noise $\sigma_0 = \sigma|\mu|^{-1/2}, \sigma_k = \sigma|1+\mu k^{-2}|^{-1/2}$ is required with the parameter σ; λ_k is an additional scaling parameter. For simplicity with $\lambda_k \equiv 1$, the dissipation effect acts as the linear Ekman damping, $-d\omega$. Together the two model parameters (d,σ) define the equilibrium variance σ_{eq}^2. The deterministic forcing is required to be zero, $\mathcal{F}_k \equiv 0$ to reach the invariant measure.

4.1.2 Statistical energy principle for the barotropic flow system

With non-zero external forcing perturbation $\delta F \neq 0$, the perturbed fluctuations (U,ω) begin to deviate from the Gaussian invariant measure p_{eq}. Still, the statistical energy principle (2.8) can be first used to describe the dynamics of total statistical energy through solving a simple scalar equation. To achieve this, we further introduce the statistical ensemble mean and disturbance about the mean state of the fluctuation variables

$$U = \bar{U} + U', \quad \omega_\mathbf{k} = \bar{\omega}_\mathbf{k} + \omega'_\mathbf{k}.$$

The statistical energy considers the combined energy in the mean and the variance in the disturbance state. Note that above the ensemble mean states $\left(\bar{U}, \bar{\omega}_{\mathbf{k}}\right)$ characterize the statistical responses in the mean due to the deterministic forcing different from the unperturbed time-averaged climate in equilibrium. The required triad symmetry (2.7) is guaranteed since the barotropic triads will only include components, $\psi_{\mathbf{k}}, \psi_{\mathbf{m}}, \psi_{\mathbf{n}}$, with the selection rule, $\mathbf{k} + \mathbf{m} + \mathbf{n} = \mathbf{0}$ [72]. Thus the nonlinear terms make no contributions in the changes of total statistical energy.

Unfortunately, neither the energy $\tilde{E}$ nor the enstrophy $\tilde{W}$ in fluctuation $\left(\tilde{U}, \tilde{\omega}\right)$ stays conserved due to the exchange of energy between the steady mean $(U_{\mathrm{eq}}, Q_{\mathrm{eq}})$. Still one important conserved quantity can be constructed as the *pseudo-energy* E_μ through a linear combination of the fluctuation energy and enstrophy $E_\mu \equiv \tilde{W} + \mu \tilde{E}$. The pseudo-energy E_μ is often more useful since it combines the two important conserved quantities. It is useful to investigate the ensemble statistics in the first two moments rather than a single trajectory realization since they not only characterize the deviations from the steady state mean, but also illustrate the evolution of uncertainty (variance) for this mean estimation. Finally we can define the *total statistical energy in fluctuations* through the original pseudo-energy as a combination of mean and variance

$$\langle E_\mu \rangle \equiv \frac{\mu}{2} \langle E_U \rangle + \frac{1}{2} \sum_{1 \le |\mathbf{k}| \le N} \left(1 + \mu k^{-2}\right) \langle E_{\mathbf{k}} \rangle, \tag{4.6}$$

with $\langle E_U \rangle = \bar{U}^2 + \overline{U'^2}$ the large-scale statistical energy and $\langle E_k \rangle \equiv |\bar{\omega}_k|^2 + \overline{|\omega_k'|^2}$ the energy in fluctuation modes.

Using the conservation law for the pseudo-energy E_μ, we are able to derive the statistical energy dynamics for the total energy $\langle E_\mu \rangle$. Accordingly the statistical energy equation with the prescribed Ekman damping and stochastic forcing in (4.5) and the non-zero deterministic forcing perturbation δF becomes

$$\frac{d \langle E_\mu \rangle}{dt} = -2d \langle E_\mu \rangle + \mu \delta F_0 \cdot \bar{U} + \sum_{\mathbf{k}} \langle \delta F_{\mathbf{k}}, \bar{\omega}_{\mathbf{k}} \rangle_\mu + Q_{\sigma,\mu}. \tag{4.7}$$

In the above scalar equation, the inner product is defined through the metric in the pseudo-energy (4.6) according to each perturbed mean, and the entire contribution from the stochastic white noises forcing is applied

$$\langle f_{\mathbf{k}}, g_{\mathbf{k}} \rangle_\mu = \left(1 + \mu k^{-2}\right) f_{\mathbf{k}}^* \cdot g_{\mathbf{k}}, \ Q_{\sigma,\mu} = \frac{1}{2} \mu \sigma_0^2 + \frac{1}{2} \sum_k \left(1 + \mu k^{-2}\right) \sigma_k^2.$$

As a find comment, only the statistical mean is included in the contribution to the total statistical energy change due to the exerted external forcing. Thus the dynamics of the total statistical energy combining mean and variance in (4.7) is determined through only the change in first order mean state together with the specific forcing and dissipation effects. One advantage of the statistical energy equations is that we can predict the total responses of second-order moments from $\langle E_\mu \rangle$ requiring only knowledge of first-order moments.

4.1.3 Numerical illustration of the flow structures

We first provide an illustration about the typical barotropic flow structures with the topographic stress. In the direct numerical simulations, the wave number truncation is kept relatively small as $N = 12$ so that the major large-scale variability is maintained. This also enables us to run direct ensemble simulations for comparison with the true statistics. The topography is taken as a zonal structure on the largest scale mode with perturbations added in smaller scales such that

$$h = H \left(\sin x + \cos x\right) + H \sum_{2 \le k \le N} k^{-2} e^{i(\mathbf{k} \cdot \mathbf{x} - \theta_{\mathbf{k}})}. \tag{4.8}$$

In the simulations we take the topographic strength $H = 3\sqrt{2}/4$ and uniform phase shift $\theta_{\mathbf{k}} = \frac{\pi}{4}$. Besides, the beta-effect is fixed as $\beta = 1$ and the linear damping uses $d = 0.1$. In the unperturbed equation, no deterministic forcing is used for all the scales $\delta F_0 = \delta F_k = 0$. A pseudo-spectral method is applied and the 4th order Runge-Kutta scheme is used for the time integration. The random noise part is added through a standard Euler-Maruyama scheme.

Figure 4.1 plots the typical flow field snapshots with different forcing perturbations $\delta F = 0, 0.5, 1$. A dominant eastward zonal flow with $U > 0$ is generated in the first case. As the forcing perturbation δF changes on the largest scale, the eastward flow gets weakened and the jet direction gets switched to the west (left) direction with $U < 0$. The abrupt change of direction in the zonal mean jet is an important observation related with more realistic geophysical flows. More discussions about the stability analysis due to topographic stress can be found in [42, 70] and next in Section 4.4.
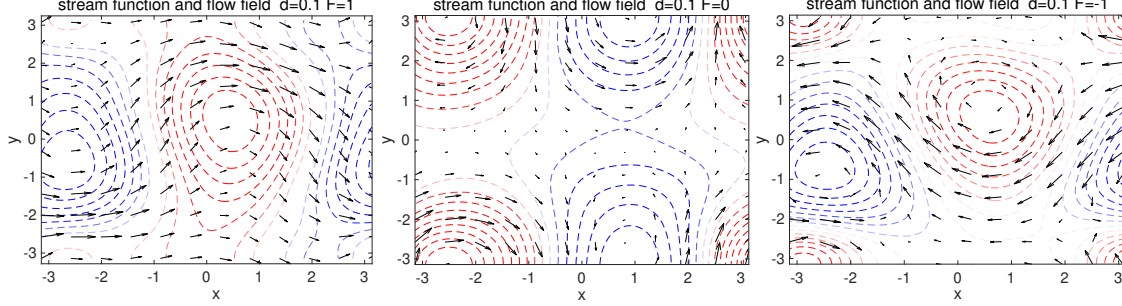
Figure 4.1: Mean stream functions (dashed contours) and the entire flow field (vector field) with different forcing strength $\delta F = 0, 0.5, 1$. The flow field shifts from eastward to blocked circulations to strong westward jet as the external forcing changes.

4.2 Linear response operators according to Gaussian invariant measure

The question in the statistical response theory asks how the distribution function p^δ differs from the unperturbed invariant density p_{eq} when inhomogeneous perturbations in different scales, $\delta F_0, \delta F_k$, are exerted. Large non-Gaussian higher order statistics could be induced even with a small perturbation forcing due to the nonlinear effects. Next, we test the extent of skills in the linear and nonlinear response predictions using information only in the unperturbed climate p_{eq}.

The linear response theory in (2.12) offers a convenient leading order approximation of the responses with the explicit formulation of the invariant measure (4.4). We focus on the first two moments of the state variables in calculating the linear response operator $\mathcal{R}_A$. Following the standard steps described in Section 2.3 using the linear response formula (2.13) and the Gaussian invariant measure (4.4) as the unperturbed equilibrium, the linear response operators for the mean state can be computed from the autocorrelation functions

$$\mathcal{R}_A(t) = \sigma_{\text{eq}}^{-2} \left[\delta f_0 \mu \left\langle A'(t) U'(0) \right\rangle_{\text{eq}} + \sum_{\mathbf{k}} \delta f_{\mathbf{k}} \left(1 + \mu k^{-2} \right) \left\langle A'(t) \omega_{\mathbf{k}}'(0) \right\rangle_{\text{eq}} \right], \tag{4.9a}$$

where $\mathcal{R}_A$ is the mean response for the large-scale state with $A = U$ and for the small-scale vortical mode with $A = \omega_{\mathbf{k}}$, subject to the general deterministic perturbation $(\delta F_0, \delta F_{\mathbf{k}})$. The total response includes contributions from all cross-correlations between different scales. In practice, we only need to focus on the perturbed directions that dominate the statistical response functionals. The linear response operators for the covariances of $A = U, \omega_{\mathbf{k}}$ can be discovered in a similar way as the lagged-in-time third order correlations between large and small scales

$$\mathcal{R}_{A^2}(t) = \sigma_{\text{eq}}^{-2} \left[\delta f_0 \mu \left\langle A'^2(t) U'(0) \right\rangle_{\text{eq}} + \sum_{\mathbf{k}} \delta f_{\mathbf{k}} \left(1 + \mu k^{-2} \right) \left\langle A'^2(t) \omega_{\mathbf{k}}'(0) \right\rangle_{\text{eq}} \right], \tag{4.9b}$$

Still, here for capturing the higher order responses in this more complex system, it is necessary to include the feedbacks from cross-correlations between different scales. Even though the cross-correlations between U and ω get decoupled in the statistical steady state, the non-zero transient response cannot be ignored due to the nonlinear dynamics.

Given hyper-ellipticity, the above system with stochastic forcing is provably geometric ergodic [56]. The statistical average under equilibrium measure can be computed through temporal average along a single trajectory, that is,

$$\left\langle f(t) g(0) \right\rangle_{\text{eq}} = \lim_{T \to \infty} \frac{1}{T} \int_0^T f(\tau + t) g(\tau) \, d\tau.$$

Exploiting this ergodicity is an effective way to reduced the computational cost. With the linear response operator $\mathcal{R}_A$ available, the leading order statistical response prediction can be computed using the FDT formulation (2.12). For simplicity, we focus on the responses to constant perturbation, $\delta \mathbf{F} = a \delta \mathbf{f}$ with the scalar a defining the amplitude of the perturbation. We only need to calculate the time-integrated value R of the linear response operator to get the linear prediction

$$\delta \left\langle A \right\rangle = \int_0^t \mathcal{R}_A(t-s) \delta F \, ds = a \int_0^\infty \mathcal{R}_A(t) \, dt. \tag{4.10}$$
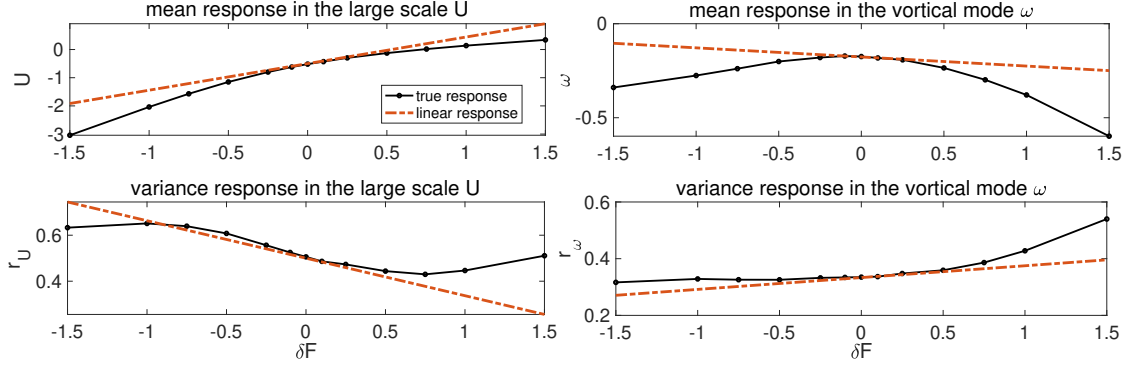
Figure 4.2: Statistical response in mean and variance in the large scale flow U and first vortical mode ω_1. The forcing perturbation amplitude ranges from -1.5 to 1.5. The true response from direct model simulation is compared with the FDT linear response predictions.

Using the above formula (4.10) for constant forcing perturbation, the leading order responses can be calculated easily and the predictions can be exact if the system is linear. On the other hand, many important nonlinear information in the integrated form of the linear response operator R_A is neglected. This will become a serious problem as the nonlinear interactions between modes grow large.

As a first test for the prediction skill of the linear response theory, deterministic forcing perturbations are added on the first two largest scale modes δF_U and δF_1. The perturbation is tested on a wide range with $a \in [-1.5, 1.5]$. The results for the responses in the mean and variance are shown in Figure 4.2. First for the true statistical responses, nonlinearity becomes dominant in both mean and variance even with small perturbation amplitudes. The linear response prediction to the constant perturbation gives a tangent line at the zero perturbation point $\delta F = 0$. It offers the infinitesimal rate of change near the origin, but fails to capture the nonlinear responses as the perturbation grows large.

4.3 Nonlinear response functionals from reduced-order statistical methods

In the prediction of nonlinear responses, reduced-order statistical models are required in correctly representing the nonlinear higher order energy transfer mechanism. Here for the topographic barotropic flow, we focus on the responses in the large scale flow U and the largest scale vortical mode ω_1 due to perturbations. Thus only the first three modes are resolved compared with the original truncated system. Following the general modeling steps in Section 3.3, the optimal model parameters are first calibrated in the training phase, then the nonlinear responses are predicted in the forecast stage.

4.3.1 Reduced-order model for the barotropic system with topography

The same model reduction strategy in (3.9) is applied here on this barotropic system. In the reduced-order statistical dynamics, we focus on the prediction in the mean $(\bar{U}, \bar{\omega})$, variance (r_U, r_ω) and the cross-covariance c. Explicitly, the dynamical equations for the statistical mean and variance in the leading modes can be derived for the imperfect reduced-order model:

- *Mean equations*:

$$\frac{d\bar{\omega}_1}{dt} + L_m = -d\bar{\omega}_1 + \delta F_1 \; - (d_{M,1} + i\omega_{M,1})\,\bar{\omega}_1 + G_M,$$
$$\frac{d\bar{U}}{dt} - i\hat{h}_1^*\bar{\psi}_1 = -d\bar{U} + \delta F_0 \; - d_{M,0}\bar{U} + H_M. \tag{4.11a}$$

- *Covariance equations*:

$$\frac{dr_{\omega,1}}{dt} + 2L_r = -2dr_{\omega,1} + k^{-2}\sigma_1^2 \; - 2d_{M,1}r_{\omega,1} + \sigma_{M,1}^2,$$
$$\frac{dr_U}{dt} + 2\hat{h}_1^*c_1 = -2dr_U + \mu^{-1}\sigma^2 \; - 2d_{M,0}r_U + \sigma_{M,0}^2, \tag{4.11b}$$
$$\frac{dc_1}{dt} + L_c = -2dc_1 \; - (d_{M,0} + d_{M,1} + i\omega_{M,1})\,c_1.$$

21

In the mean equations, L_m represents the quasi-linear part as well as the large-small scale interaction, G_M and H_M add the correction from the unresolved subspace using equilibrium statistics. In the variance equations, L_r and L_c represent the quasi-linear effects between the small and large scale variables. The last terms on the right hand sides of the equations offer the imperfect model estimation of the unresolved higher order feedbacks. Detailed derivation and expressions of the above statistical equations can be found in [68].

The same model reduction strategy in (3.9) is carried out for this barotropic system. Feedbacks from higher-order statistics through nonlinear triad interactions are replaced by the corrections as in (3.10). Imperfect model parameters $(d_M, \omega_M, \sigma_M)$ are introduced for each scale to control the model performance. The information-theoretic framework (3.5) is applied in the training stage for the optimal model parameters. In addition, the model sensitivity is improved by scaling the parameters with the total statistical energy $\langle E \rangle$ by solving the statistical energy equation (4.7) requiring only the statistical mean state with perturbation. The total energy scaling factor has been shown crucial for the accurate prediction of model responses.

4.3.2 Reduced model performance in predicting nonlinear responses

In the training phase, the imperfect model parameters are determined based on first equilibrium consistency to recover the exact equilibrium statistics in the unperturbed climate; and then model sensitivity in reproducing the linear response operators using the reduced statistical model. First, the equilibrium consistency is guaranteed using the steady state mean and variance to compute the equilibrium higher order moment feedbacks. This offers the first constraint on the model parameters. Next, the model sensitivity is improved by tuning the rest model parameters according to the linear response operators $\mathcal{R}$ for the mean and variance in (4.9a) and (4.9b). The relative entropy distance offers an unbiased metric to calibrate the model error combining the mean and variance.

The optimal tuning results for the linear response operators $\mathcal{R}_A(t)$ for the mean and variance in the largest scale states are compared in the first part of Figure 4.3. The optimized reduced-order model shows high skill in recovering the linear response operators for both the mean and variance. Next in the second part of Figure 4.3, the predictions for the nontrivial nonlinear responses in mean and variance are shown. The same constant forcing perturbations with different amplitudes as in Figure 4.2 are tested again for the efficient reduced order model. In this case, the strong nonlinear responses appearing in both mean and variance are captured with desirable accuracy in the nonlinear statistical model. This example together with the previous linear response prediction with much larger errors emphasizes the crucial role in modeling the important higher order moment feedbacks in achieving accurate prediction for the nonlinear statistical responses.

4.4 Rigorous statistical bounds for the total statistical responses

Using the statistical reduced-order models, the nonlinear responses along the most important model directions can be predicted with accuracy. From another perspective, it is also useful to investigate the bounds in the total statistical variability of the turbulent system. This is related with the statistical saturation bounds concerning the nonlinear stability. In this last section, we display the major conclusions developed in [70] for the rigorous statistical bounds in the barotropic model with topography.
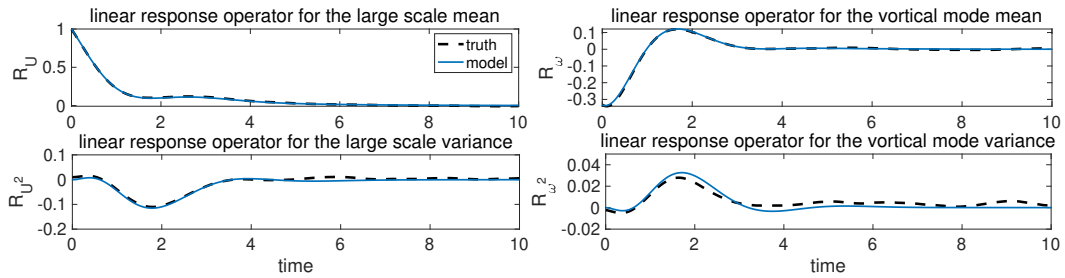
In the previous discussions for linear response theory, the fluctuation components about the steady state solution $(U_{\text{eq}}(\mu), \Psi_{\text{eq}}(\mu))$ are characterized by the Gaussian invariant measure (4.4). This invariant distribution becomes unrealizable when the linear dependence parameter μ changes to negative. In this scenario, one natural question is how the system responds to such uncertainties in the unstable regimes $\mu < 0$.

### 4.4.1 Statistical energy saturation bounds in response to forcing and dissipation

The statistical saturation bounds in general are subject to two classes of flow perturbations: the perturbations in the initial distribution configuration; and the external forcing and dissipation effect. The two sources of uncertainties are unified under the same analytical framework using the conservation of statistical pseudo-energy (4.6) in [70]. Here we stick to the previous model setup with the forcing and damping forms (4.5), and provide the saturation bounds in fluctuation responses subject to external perturbations.

The total statistical energy $\langle E_\mu \rangle$ in fluctuation due to the Ekman damping and forcing effects follows the dynamical equation (4.7)

$$\frac{d\langle E_\mu \rangle}{dt} = -2d\langle E_\mu \rangle + \mu \bar{U} \cdot \delta F_0 + \sum \left(1 + \mu k^{-2}\right) \delta \hat{F}_{\mathbf{k}}^* \cdot \bar{\omega}_{\mathbf{k}} + Q_{\sigma,\mu},$$

22

(a) linear response operators for the mean and variance
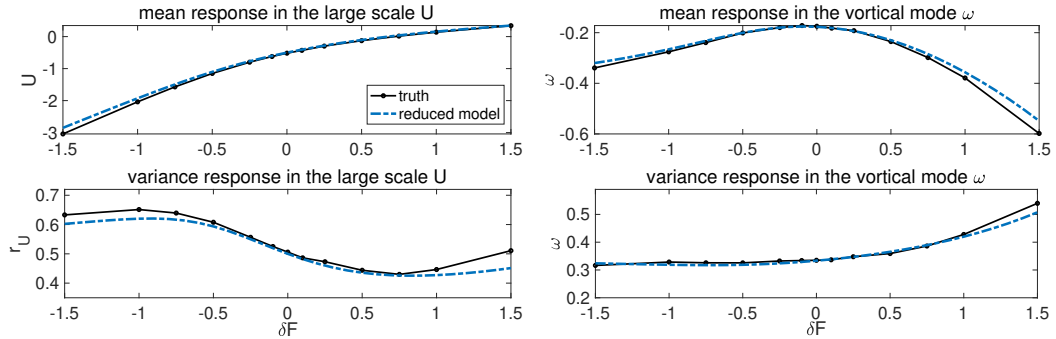
(b) prediction for the mean and variance responses

Figure 4.3: Prediction of the nonlinear statistical responses in the mean and variance for the topographic barotropic flow from the reduced-order model. The upper panel shows the model prediction for the linear response operators for the mean and variance in the training stage; the lower panel displays the reduced model predictions for the mean and variance responses due to different deterministic forcing perturbations.

with the deterministic part applying on the statistical mean state and the stochastic part offering the combined contribution through $Q_{\sigma,\mu}$. To find the proper bound of the total statistical energy due to the external forcing, we separate the interaction terms with the statistical mean by applying Cauchy's inequality

$$\left(1 + \mu k^{-2}\right) \delta F_{\mathbf{k}}^* \cdot \bar{\omega}_{\mathbf{k}} < (4\lambda)^{-1} \left|1 + \mu k^{-2}\right| \left\langle |\omega_{\mathbf{k}}|^2 \right\rangle + \lambda \left|1 + \mu k^{-2}\right| |\delta F_{\mathbf{k}}|^2,$$

$$\mu \delta F_0 \cdot \bar{U} < (4\lambda)^{-1} |\mu| \left\langle U^2 \right\rangle + \lambda |\mu| \delta F_0^2.$$

with parameter $\lambda > 0$. Using *Grönwall's inequality* to the above relations, the saturation bound for the total statistical energy $\langle E_\mu \rangle$ due to the effect of damping and external forcing can be found as

$$\langle E_\mu \rangle = \frac{\mu}{2} \left\langle U^2 \right\rangle + \frac{1}{2} \sum_{1 \le k \le N} \left(1 + \mu k^{-2}\right) \left\langle |\omega_{\mathbf{k}}|^2 \right\rangle \le C_\mu, \tag{4.12}$$

with the statistical bound $C_\mu = \frac{\mu}{2} \left(\left(d^{-1} F_0\right)^2 + d^{-1}\sigma_0^2 \right) + \frac{1}{2} \sum \left(1 + \mu k^{-2}\right) \left(\left|d^{-1} F_{\mathbf{k}}\right|^2 + d^{-1}\sigma_{\mathbf{k}}^2 \right)$. The result in (4.12) offers a desirable bound for the stable regime $\mu > 0$. However with $\mu < 0$, one obvious difficulty is that the components in the statistical energy $\langle E_\mu \rangle$ are not all positive. Thus (4.12) is no longer a saturation bound for the total energy, but a balance between the positive and negative subspaces that separate the total $\langle E_\mu \rangle$.

The trick in [70] is to propose 'reference states' with parameter $\alpha > 0$ but with the real forcing in the form with parameter $\mu < 0$. The previous bound (4.12) is still valid according to the reference state energy $\langle E_\alpha \rangle$, which remains positive definite in all coefficients of $\langle U^2 \rangle, \langle |\omega_{\mathbf{k}}|^2 \rangle$. Additional 'reference forcing' effects need to be separated for the dynamical equation of E_α based on the reference state with parameter $\alpha > 0$ in the mean flow and vortical modes. Then the final saturation bound for the unstable regime $\mu < 0$ is achieved by minimizing among all the bounds in (4.12) with the reference states $\alpha > 0$. We state the final conclusion for the saturation bounds with forcing and dissipation effects in the following theorem:

Theorem 4. *(Saturation bound for statistical mean and variance with damping and random forcing) With the linear damping and forcing as in (4.5), the combined statistical mean fluctuation and variance, $\theta E^m + E^v$, with the ratio parameter $0 \le \theta < 1$ can be controlled as in*

$$\theta E^m + E^v \le C_\mu^\theta, \tag{4.13}$$

with saturation bound

$$C_\mu^\theta = \min_{\alpha > 0} \frac{1}{1 - \theta} \left[\frac{(\alpha - \mu)^2}{\alpha^2} \frac{\beta^2}{\mu^2} + \sum_k \frac{(\alpha - \mu)^2 k^2}{\alpha(\alpha + k^2)} \frac{|\hat{h}_{\mathbf{k}}|^2}{(\mu + k^2)^2} \right] + d^{-1} \left[\sigma_U^2 + \sum_k \left(k^{-2} + \alpha^{-1}\right) \sigma_{\mathbf{k},0}^2 \right].$$

Above $E^m = \bar{U}^2 + \sum k^2 |\bar{\psi}_{\mathbf{k}}|^2$ is the total statistical energy in mean fluctuation, and $E^v = \overline{U'^2} + \sum k^2 \overline{|\psi'_{\mathbf{k}}|^2}$ is the total variance in the flow fluctuation.

4.4.2 Numerical verification of the saturation bounds

The saturation bound in (4.13) can be verified through simple numerical simulations. The basic model setup is kept the same as before. The forcing perturbation is added according to the reference steady state $(U_{\text{eq}}, \Psi_{\text{eq}})$ defined by μ. The maximum statistical growth in mean perturbation and variance is tested in the statistically unstable range $\mu \in (-2, -1)$. Figure 4.4 compares the total statistical energy in the mean and variance fluctuation through direct numerical simulations and the theoretical saturation bound (4.13) in the total variability of the statistics. The saturation bound offers a tight upper limit for the maximum growth in the total statistics in both the mean fluctuation and the variance. Especially, for the combined mean fluctuation and variance bounds with two ratio values θ, the upper bound estimation is extremely close to the numerical results, offering an accurate prediction for the maximum increase in the total statistical energy. A more complete discussion with many different forcing scenarios for the statistical saturation bounds according to both initial uncertainty and external forcing excitations can be found in [70].

5 Beating the Curse of Dimensionality using Statistical Control Theory for Complex Systems

The statistical control of inhomogeneous turbulent systems offers another set of problems where the statistical response theory can play an important role. The efficient control of complex systems remains a challenging problem due to the
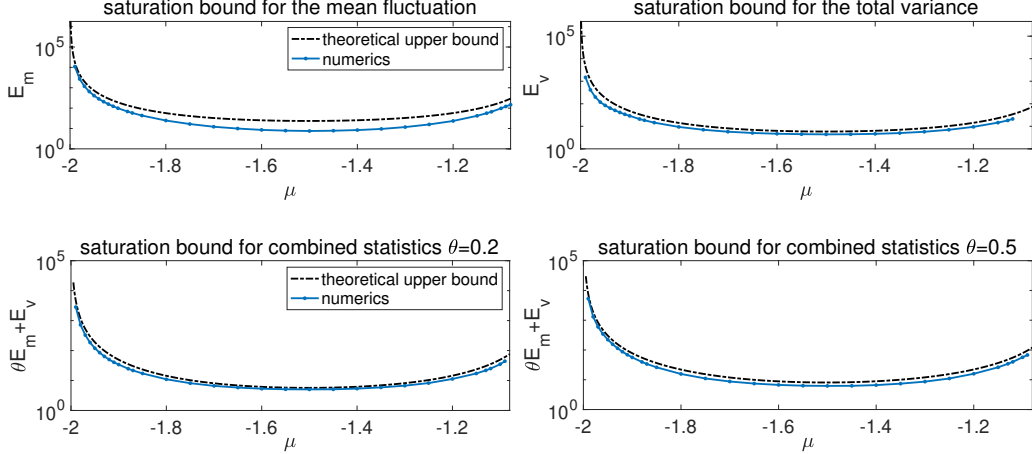
Figure 4.4: Statistical saturation bounds with damping and forcing perturbation in the unstable regime $\mu \in (-2, -1)$. The first row shows the bounds in the energy in mean fluctuation and total variance separately, and the second row gives the combined statistical bounds with different parameter values θ. The theoretical bounds are compared with direct numerical simulations.

inherent nonlinearity, high-dimensionality, and strong exchange of energy between scales [8, 38, 63, 23]. The major goal of the control theory can be summarized as to construct an optimal course of action (the *control*) to drive the perturbed statistical solution of a complex turbulent system back to the small neighborhood of the original unperturbed target statistical equilibrium state.

One successful approach for controlling flows in the transition to turbulence is dynamical programing by solving the *Hamilton-Jacobi-Bellman* (HJB) equation [3, 5]. However, the curse of dimensionality appears during directly solving this HJB PDE when the system becomes genuinely high dimensional and fully turbulent [45]. We have shown previously in Sections 4 that the statistical response theory offers an efficient way to characterize the model sensitivity to perturbations with robust performance, so that it enables us to construct an alternative approach for the specific control without the need to run the specific complex system. In this section, we illustrate the ideas presented in [54, 55] for the effective control combining the statistical energy principle and statistical response theory. The topographic barotropic model (4.1) is used as a typical example to demonstrate the novel control strategy and its skill.

5.1 Efficient control of total statistical energy with mean response

To avoid directly controlling the high dimensional system (2.1), we first seek to control the scalar statistical energy (2.8) through manipulating the mean responses $\delta \bar{\mathbf{u}} = \bar{\mathbf{u}} - \bar{\mathbf{u}}_{\mathrm{eq}}$ subject to various perturbation forcing $\delta \mathbf{F}$

$$\frac{dE'}{dt} - 2dE' + \bar{\mathbf{u}}_{\mathrm{eq}} \cdot \delta \mathbf{F} + \bar{\mathbf{F}}_{\mathrm{eq}} \cdot \delta \bar{\mathbf{u}} + \delta \bar{\mathbf{F}} \cdot \delta \bar{\mathbf{u}} + \delta \bar{\mathbf{F}} \cdot \delta \bar{\mathbf{u}}, \quad E'(t) = E(t) - E_{\mathrm{eq}}.$$

In the control problem, the focus is on the statistical energy fluctuation $E' = E - E_{\mathrm{eq}}$ removing the unperturbed equilibrium E_{eq} with $\delta \mathbf{F} \equiv 0$. Instability will not appear in this statistical energy equation due to the symmetry in the nonlinear interactions [44, 45]. Thus the major difficulty in stabilizing many directions of instability in controlling the original equation is circumvented.

Next, The (deterministic) control forcing and the equilibrium statistics are projected to the subspace for control spanned by a truncated orthonormal basis $\{\mathbf{e}_k\}_{k=1}^N$

$$\delta \mathbf{F} \equiv \vec{\kappa}(t) = \sum_{k=1}^M \kappa_k(t) \mathbf{e}_k, \ \bar{\mathbf{u}}_{\mathrm{eq}} = \sum_{k=1}^N \bar{u}_{\mathrm{eq},k} \mathbf{e}_k, \quad \bar{\mathbf{F}}_{\mathrm{eq}} = \sum_{k=1}^N \bar{F}_{\mathrm{eq},k} \mathbf{e}_k,$$

where the control forcing $\vec{\kappa}(t)$ applies on the selected $M < N$ leading modes. The statistical energy fluctuation equation with leading order responses in the mean can be written with respect to the forcing perturbation along the orthonormal

modes $\{\mathbf{e}_k\}_{k=1}^M$

$$\frac{dE}{dt} = -2dE(t) + \sum_{k=1}^M \left[\bar{u}_{\text{eq},k} \cdot \kappa_k(t) + \bar{F}_{\text{eq},k} \cdot \delta\bar{u}_k(t;\vec{\kappa}) \right], \quad E(0) = E_0. \tag{5.1}$$

Above and later the primes for the fluctuation components are dropped in the statistical energy fluctuation E', and E_0 is the initial total statistical energy perturbation to be controlled. Only leading order terms $O(\delta)$ remains in the dynamics by assuming the perturbation is kept relatively small.

At last, we link the mean responses $\delta\bar{u}$ with the control forcing perturbation κ using the linear response theory. Through the linear response formula in (2.12), the response in the leading order mean state, $\delta\bar{\mathbf{u}}$, subject to the external forcing $\vec{\kappa}(t)$ can be estimated using the mean response operator $\mathcal{R}_u$

$$\delta\bar{u}_k(t) = \int_0^t \mathcal{R}_{u,k}(t-s)\,\kappa_k(s)\,ds, \quad \mathcal{R}_{u,k}(t) = \langle u_k(t)\,u_k(0)\rangle / r_{\text{eq},k}.$$

Above we assume that the responses from diagonal components for the variance along each direction $\mathbf{e}_k$ is dominant, and cross-covariances between different mode can be neglected. The diagonal model with autocorrelation functions as the linear response operator for the mean $\mathcal{R}_u$ can be shown as an attractive option from judicious simple linear regression approximations [51, 66, 69].

Using the linearization in both the statistical energy equation and the leading order mean response, the first control problem for the total statistical energy fluctuation can be formulated using the mean response operator $\mathcal{R}_u(t)$. The *statistical control equation in leading order responses* can be rewritten from the original statistical dynamics as

$$\frac{dE}{dt} = -2dE(t) + \sum_{k=1}^M \left[\bar{u}_{\text{eq},k} \cdot \kappa_k(t) + \bar{F}_{\text{eq},k} \cdot \int_0^t \mathcal{R}_{\bar{u},k}(t-s)\,\kappa_k(s)\,ds \right], \quad E(0) = E_0. \tag{5.2}$$

The control system (5.2) is linear but involves nonlinear statistical functionals as coefficient from the target unperturbed equilibrium measure. *Non-Markovian forcing* is introduced through the linear response operator $\mathcal{R}_k$.

5.2 Effective statistical control strategy in two steps

The task now is to find proper formula for the ideal *optimal control forcing* $\vec{\kappa}(t)$ on the mean state to drive the perturbed energy fluctuation E in (5.2) back to zero (or close to zero) efficiently with minimum cost. A *local statistical control* $\mathcal{C}(t)$ is then introduced as a nonlocal functional of the scalar control forcing $\vec{\kappa}(t)$ containing all the perturbed feedbacks in the statistical energy fluctuation. We first construct the linear statistical control problem by proposing a proper cost function to optimize. With the statistical control $\mathcal{C}(t) = \sum_k \mathcal{C}_k$ defined with a combination of the contributions from each mode $\mathbf{e}_k$, the control system (5.2) is converted to the linear scalar dynamical equation between time interval $[t, T]$

$$\frac{dE}{ds} = -2dE(s) + \sum_k \mathcal{C}_k(s), \quad E(t) = x,\ t \le s \le T, \tag{5.3}$$

regardless of the specific structure in the functional $\mathcal{C}(t)$. We attempt to minimize the *cost function* as a quadratic combination of the energy fluctuation E and control functional in each mode $\mathcal{C}_k$

$$\mathcal{F}_\alpha \left[\mathcal{C}_k(\cdot) \right] \equiv \int_t^T \left[E^2(s) + \sum_{k=1}^M \alpha_k \mathcal{C}_k^2(s) \right] ds + k_T E^2(T), \tag{5.4}$$

The weighting parameter $\alpha_k > 0$ is introduced to add a balancing factor between the control efficiency (due to E) and the control expense (due to $\mathcal{C}_k$). In this way, we need just focus on this statistical control operator $\mathcal{C}(t)$ for total statistical energy $E(t)$ in the first step regardless of the explicit forms of the mean state and specific forcing perturbations or exact equilibrium statistics. Then in the second step, the task is to invert the (nonlocal) functional $\mathcal{C}(t)$ to get the explicit forcing control strategy for $\kappa(t)$ using the leading order mean responses.

5.2.1 Optimal control on statistical energy identity

In the first step of constructing statistical control $\mathcal{C}(t)$ in (5.3), this linear statistical control problem can be directly solved by the HJB equation through *dynamic programming* [3]. It solves the backward equation in time about the optimal value function $v(x,t) = \min_{\mathcal{C}} \mathcal{F}_\alpha [\mathcal{C}(\cdot)]$. The HJB equation becomes the *Riccati* equation [18, 54] that is easy to solve for the explicit optimal solution. The optimal feedback control $\mathcal{C}_k^*(t)$ together with the optimal control statistical equation for E^* can be found by the following system

$$\mathcal{C}_k^*(t) = -\alpha_k^{-1} K(t) E^*(t), \; E^*(t) = E_0 \exp\left(-2dt - \sum_k \alpha_k^{-1} \int_0^t K(s)\, ds\right),$$

$$\frac{dK}{dt} = \sum_k \alpha_k^{-1} K^2 + 4dK - 1, \quad 0 \le t < T,$$

(5.5)

with the final time value $K(T) = k_T$ and initial fluctuation energy $E^*(0) = E_0$.

5.2.2 Attribution of the optimal statistical control

The second step of the problem is to find the optimal control forcing $\kappa_k(t)$ from the optimal statistical control $\mathcal{C}^*(t)$ achieved. Through the explicit formula (5.2), the attribution of the optimal statistical control forcing κ becomes the nonlinear inversion using the linear response factor $\mathcal{R}_u$

$$\mathcal{C}^*(t) = \bar{u}_{\text{eq}} \kappa^*(t) + \bar{F}_{\text{eq}} \int_0^t \mathcal{R}_u(t - s)\, \kappa^*(s)\, ds,$$

(5.6)

Combining the above equality (5.6) with the previous explicitly optimal statistical control (5.5), it requires an explicit expression for the mean response operator $\mathcal{R}_u$ so that the nonlocal operator can be inverted. The mean response function can be simply approximated by the autocorrelation using a linear regression model

$$\mathcal{R}_u^M(t) = \exp\left(-\gamma_M t\right) = \exp\left[-(d_M + i\omega_M)t\right].$$

(5.7)

The imaginary parameter ω_M is used to approximate the oscillatory structure that is common in autocorrelations. The information-theoretic framework [66, 69] again offers an efficient way to reach the optimal model parameters with high accuracy. We offer some more details about the strategy in finding the optimal model parameters in (5.7) in the next section

With the approximation in the mean response operator (5.7), the explicit control forcing in (5.6) can be recovered by solving the following equation

$$\frac{d\kappa}{dt} + \left(d_M + \bar{F}_{\text{eq}}/\bar{u}_{\text{eq}}\right) \kappa(t) + \left[(d_M + 2d)K(t) - 1\right]/\alpha\bar{u}_{\text{eq}} E^*(t) = 0.$$

(5.8)

By solving the above equation, the proposed control $\kappa(t)$ is constructed in explicit form to force the perturbed system back to the neighborhood of initial unperturbed climate. The detailed derivation of the above steps can be found in [55].

In summary, the two-step strategy of the statistical control has the advantage of only requiring equilibrium information *a priori* without running the detailed high-dimensional complex turbulent system with perturbations. The linear response operator $\mathcal{R}_u$ for the mean can be approximated using the autocorrelation function in the most sensitive direction. Therefore the entire control strategy can be carried out easily despite the highly complicated original turbulent dynamical system in a large phase space with instability.

5.3 Statistical control of the topographic barotropic flow

The statistical control strategy is displayed under the topographic barotropic turbulent model (4.1) with the same model setup. As shown in the various tests in Section 4, the flows show distinct inhomogeneous divergence from the equilibrium state with changing directions as forcing perturbation is exerted. In controlling the turbulent flow, we again assume that the equilibrium state $(U_{\text{eq}}, \omega_{\text{eq}})$ (i.e. the climate) is known with reasonable accuracy, and the goal is to find the optimal control (as one external forcing) that can drive the perturbed states (say, due to unknown climate change perturbation δF) back to the unperturbed equilibrium at a fast rate.

According to the general framework, we begin with the scalar statistical dynamical equation to derive a optimal statistical control $\mathcal{C}(t)$. Then the the optimal control forcing κ is found by solving a scalar Riccati equation regardless of the complicated nonlinear effects. The same statistical energy equation (4.7) is adopted for the construction of statistical control $\mathcal{C}(t)$ as in (5.3). As in the previous simulations, the perturbation forcing is only exerted on the large scale flow U and the largest topographical modes ω_1. These are the most sensitive directions to perturbations according to the linear response analysis in Section 4.2. Therefore, we just need to control on the total statistical energy fluctuation using control $\mathcal{C}_0$ on the mean flow U and $\mathcal{C}_1$ on the ground vortical mode ω_1

$$\frac{d\langle E \rangle}{dt} = -2d \langle E \rangle + 2\mathcal{C}_1 + \mathcal{C}_0.$$

The optimal energy control can be found using the solution in (5.5)

$$\mathcal{C}_0 = -\alpha_0^{-1} K(t) \langle E \rangle (t), \quad \mathcal{C}_1 = -\alpha_1^{-1} K(t) \langle E \rangle (t).$$

The values of α_0, α_1 can be determined by the energy in mean flow U and mode ω_1.

5.3.1 Linear approximation for the statistical responses in perturbed modes

The next task is to recover the explicit control forcing $\kappa(t)$ with the inversion relation through the statistical control solutions $\mathcal{C}_0, \mathcal{C}_1$. The first-order response is approximated by the autocorrelation functions so that

$$\delta \bar{u}(t) = \int_0^t \mathcal{R}_u(t-s) \kappa(s) \, ds = r_u^{-1} \int_0^t \langle u(t-s) u(0) \rangle \kappa(s) \, ds,$$

with $u = U$ controlling the large-scale flow and $u = \omega$ controlling the small-scale vortical modes. As a further approximation for practical computation, linear regression model is used to fit the autocorrelations, that is, $\mathcal{R}_U^M(t) = \exp\left(-\gamma_0^M t\right)$ and $\mathcal{R}_\omega^M(t) = \exp\left(-\left(\gamma_1^M - i\omega_1^M\right) t\right)$. The first row of Figure 5.1 gives the linear model fitting for the autocorrelation functions. Good agreement is reached using the linear explicit fitting functions. This guarantees the feasibility to recover the control forcing form by solving the inversion problem (5.6). More applications of this linear fitting of the response operator will be shown next in Section 6 for the prediction of intermittency.

5.3.2 Verification of the statistical control in the perturbed barotropic flow

In the numerical test, the same setup as in Section 4.1 is adopted again for the control tests. The unperturbed equilibrium is reached with no additional forcing $\delta F_0 = \delta F_1 = 0$, while perturbations are added on the largest scales, $\delta F_0 = dF, \delta F_1 = dF$. Still all the rest uncontrolled modes in smaller scales count for large percentage of the total energy, thus are crucial in the final flow structure.

In the verification step, the skill of the optimal control forcing (κ_0, κ_1) is applied to the perturbed flow at time $t = 5$. The lower panel of Figure 5.1 gives the control results compared with uncontrolled case where the forcing perturbation is simply removed. The mean and variance responses in the large scale U and first mode ω_1 both converge to the unperturbed state. Compared with the uncontrolled case, the control forcing κ effectively speeds up the convergence process to a much faster rate. This illustrate the effectiveness of the efficient statistical control strategy to propose the explicit control forcing valid for high dimensional turbulent systems with many degrees of internal instability and uncertainty.

6 Predicting Extreme Events and Tracer Statistics in the Passive Scalar Turbulence

Turbulent diffusion and intermittency form another rich group of highly nontrivial multiscale problems requiring strategies using the statistical response theory [49, 61, 21, 69]. Intermittent phenomena in passive scalar turbulence refer to the bursts of extreme values followed by low-amplitude phases that are representative in the observational data [62, 65, 20]. Even with no positive Lyapunov exponents, exactly solvable models have shown to exhibit intermittent behaviors from rigorous analysis [57].

Linear and nonlinear response theories provide effective calibration strategies for the statistically accurate prediction of these extreme events. Here we illustrate the application of statistical response theory developed in [58, 57] for the prediction of intermittency under the framework of the two-layer baroclinic model (2.9e). The more complicated two-layer model is picked here due to its wider range of representative features for typical intermittency in ocean and atmosphere regimes [72, 76, 83].
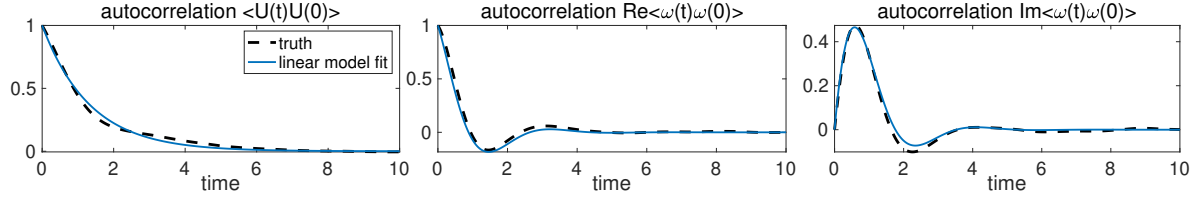
(a) fitting of the autocorrelation functions in the principle directions
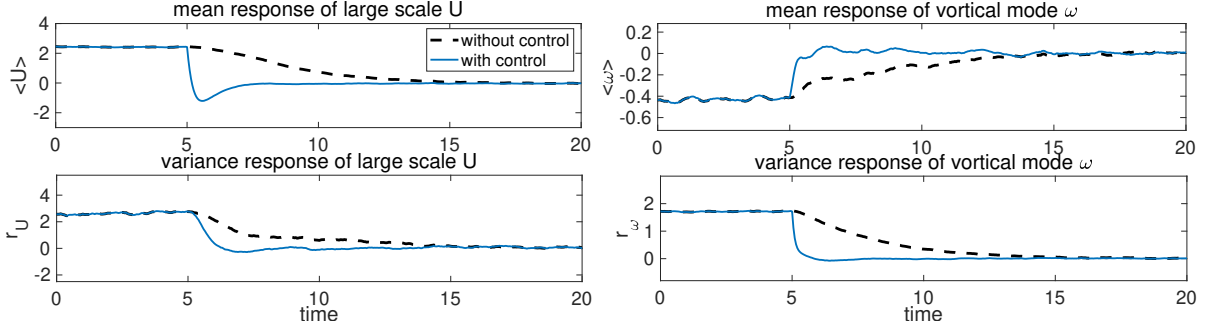
(b) verification of the control performance

Figure 5.1: Control of the topographic barotropic model. The upper panel shows the fitting the of the autocorrelation functions in the leading modes; and the lower panel gives the control results in mean and variance for the most sensitive directions.

6.1 Stochastic formulations for the passive scalar turbulence

The scalar field $T(\mathbf{x}, t)$ is characterized by the concentration of the passive tracers which immerse in the turbulent fluid with velocity $\mathbf{v}$ but do not inversely influence the dynamics of the fluid. The evolution of the scalar field is described through the joint effect of turbulent advection and diffusion [72, 75, 52]

$$\frac{\partial T}{\partial t} + \mathbf{v} \cdot \nabla T = -d_T T + \kappa_T \Delta T. \tag{6.1}$$

The dissipation is set as a linear damping and diffusion, where d_T has a stronger effect on the large-scale modes and κ_T applies to the small-scale modes for the diffusion. The statistical description of tracer transport in turbulent flows is a prevalent concern in atmospheric and oceanic fluid dynamics when the advection flow $\mathbf{v}$ becomes turbulent [75, 67]. There exists well developed statistical-dynamical understanding for the above problem but with much simpler master equations for the advection flow [57, 78]. The dynamics of the passive tracers can be also investigated via the Lagrangian approach tracking the tracer trajectories [60, 52].

6.1.1 Equations of the passive tracer turbulence with mean gradient

The existence of a background mean gradient for the tracer field has been shown responsible for many important phenomena [4, 7]. A background mean gradient varying along y direction is then introduced in the tracer field

$$T(\mathbf{x}, t) = \alpha y + T'(\mathbf{x}, t). \tag{6.2}$$

The fluctuation part of the tracer T' satisfies the following dynamics by substituting the decomposition (6.2) into the original tracer equation (6.1)

$$\frac{\partial T'}{\partial t} + \mathbf{v}(\mathbf{x}, t) \cdot \nabla T'(\mathbf{x}, t) = -\alpha v(\mathbf{x}, t) - d_T T' + \kappa_T \Delta T'. \tag{6.3}$$

The turbulence flow $\mathbf{v} = (u(\mathbf{x}, t), v(\mathbf{x}, t))$ is the solution of the two-layer equations (2.9e).

The equations (6.3) offer a detailed illustration about the energy exchange mechanism between the tracer and underlying flow field. Explicit solutions for the mean, variance, and cross-covariance between tracer and flow modes can be derived

29

explicitly and intermittency can be predicted through the random resonance between modes of the turbulent velocity and the passive tracer [57]. The system (6.3) advected by the two-layer flow contains more realistic features with inherent internal instability and strong non-Gaussian statistics. The reduced-order model is then constructed with a careful calibration according to the true model nonlinear responses.

6.1.2 Reduced-order stochastic model for the passive tracer turbulence

Usually high computational cost is required to resolve the tracer equation (6.3) as well as the complex turbulent advection flow (2.9e) through direct methods. As a continuation of the idea for model reduction in Section 3.3 and [39], we adopt the model reduction procedure with linear corrections to approximate the advection flow field in the leading M most energetic modes so that the principal variability can be captured.

First, the flow potential vorticity q_j and passive tracer disturbance T'_j can be written in the expansion under modes as

$$q = \sum_{k=1}^{N} \hat{q}_{\mathbf{k}} e^{i\mathbf{k}\cdot\mathbf{x}}, \quad T' = \sum_{k=1}^{N} \hat{T}_{\mathbf{k}} e^{i\mathbf{k}\cdot\mathbf{x}}.$$

It has been shown that important non-Gaussian and intermittent structures in the tracer field can be generated from a simplified linear Gaussian advection flow. Therefore the reduced-order advection flow equations can be proposed using the imperfect model reduction idea as in Section 3.3 and 4 to replace the complex quadratic interaction with equivalent linear damping and noise

$$d\hat{q}_{M,\mathbf{k}} = -\left(\gamma_{q,\mathbf{k}} + i\omega_{q,\mathbf{k}}\right)\hat{q}_{M,\mathbf{k}}dt - D_{q,\mathbf{k}}^M \hat{q}_{M,\mathbf{k}}dt + \Sigma_{q,\mathbf{k}}^M dW_{q,\mathbf{k}}, \quad 1 \le |\mathbf{k}| \le M. \tag{6.4}$$

The turbulent velocity field can be achieved from the streamfunction $\mathbf{v}_M = \nabla^\perp \psi_M$. Only the first $M \ll N$ large-scale modes, $1 \le |\mathbf{k}| \le M$, are resolved in the reduced-order formulation in (6.4). $(\gamma_{q,\mathbf{k}}, \omega_{q,\mathbf{k}})$ are the linear dissipation and dispersion operators. Additional damping and noise $\left(D_q^M, \Sigma_q^M\right)$ are introduced to correct model errors due to the neglected nonlinear interactions in the flow equations, so that consistent equilibrium statistics in first two moments and optimal linear response functional can be recovered.

Next, the tracer dynamics is modeled directly without additional model calibrations about the tracer field statistics in case of over fitting about data

$$d\hat{T}_{M,\mathbf{k}} + \left(\mathbf{v}_M \cdot \nabla \hat{T}_M\right)_{\mathbf{k}} dt = i\alpha k_x \psi_{M,\mathbf{k}}dt - \left(\gamma_{T,\mathbf{k}} + i\omega_{T,\mathbf{k}}\right)\hat{T}_{M,\mathbf{k}}dt, \quad 1 \le |\mathbf{k}| \le M. \tag{6.5}$$

Consistent with the advection flow model (6.4), only the first leading modes $|\mathbf{k}| \le M \ll N$ are resolved in the tracer approximation model. The advection flow solution $\mathbf{v}_M = \nabla^\perp \psi_M$ is solved from the Gaussian linear model solution in (6.4), The damping and dispersion operators are $\gamma_{T,\mathbf{k}} = d_T + \kappa_T |\mathbf{k}|^2$, and $\omega_{T,\mathbf{k}} = k_x U$ due to the dissipation and advection in large-scale zonal mean flow.

In this modeling process, we only consider the calibration about the advection flow field, and the flow solution is applied to the tracer equations for predicting tracer statistics directly. One crude approximation in flow equation (6.4) is to replace the nonlinear advection with linear damping and noise $\left(D_q^M, \Sigma_q^M\right)$ as discussed in Section 4 and previous works [66, 57]. Using the statistical formulation (3.9), the additional damping and noise corrections for the reduced-order flow vorticity model (6.4) is proposed in the following form

$$D_{q,\mathbf{k}}^M = -\frac{1}{2}Q_{F,\text{eq},\mathbf{k}}^{q,-}\left(R_{\mathbf{k},\text{eq}}^q\right)^{-1} + D_M^{\text{add}}, \quad \Sigma_{q,\mathbf{k}}^M = \left(Q_{F,\text{eq},\mathbf{k}}^{q,+} + \left(\Sigma_{M,\mathbf{k}}^{\text{add}}\right)^2\right)^{1/2}. \tag{6.6}$$

Above $Q_{F,\text{eq}}^q$ is the nonlinear flux (3.10) from the equilibrium statistics, and the parameters $\left(D_{q,\mathbf{k}}^M, \Sigma_{q,\mathbf{k}}^M\right)$ are additional corrections. Comparing with the exact true system, the reduced-order approximation is equivalent to replacing the nonlinear interaction terms with the judiciously calibrated damping and noise (6.6) in consideration with both the equilibrium energy transfer mechanism and further sensitivity correction. Still this approximation may introduce large model errors due to neglecting the feedbacks from the unresolved smaller scale fluctuations. Next, the imperfect model error is calibrated and minimized using the information-theoretical framework by calibrating the linear response functionals.

6.2 Predicting extreme events using the statistical response theory

6.2.1 Training phase for optimal linear response with information theory

Now we describe the model calibrations for consistency in equilibrium moments, and model optimization using linear response theory under a systematic information-theoretic framework. This information-theoretic framework has been utilized to systematically improve model fidelity and sensitivity and to make an empirical link between model fidelity and forecasting skill. Using the statistical response theory, proper imperfect model parameters can be proposed according to the detailed model calibration using equilibrium statistics.

Especially in the case for capturing model intermittency with fat-tailed distributions in the leading modes, accurate characterization about the transient state with instability becomes crucial. It is realized that with only the corrections from the equilibrium nonlinear interactions, large errors may still exist in the reduced-order model predictions since the autocorrection functions are not well characterized). As illustrated in the linear response theory (2.12), the mean sensitivity in the stochastic process for $q(t)$ can be approximated by its autocorrelation functions

$$\mathcal{R}_u^q(t) \equiv \langle (q(t) - \bar{q})(q(0) - \bar{q}) \rangle_{\text{eq}}. \tag{6.7}$$

Next we follow the general strategy introduced in [66, 69] for measuring autocorrelation functions with the help of information theory.

The problem here is about to find a proper metric to measure the errors in the imperfect model autocorrelation functions in the training phase in a balanced way. A preferable measure to offer an unbiased metric for the imperfect model probability distribution p_M from the truth p is to use the relative entropy (3.5) concentrating on the leading order moments. However one additional difficulty in tuning the autocorrelation functions under the information metric is that the functions given in (6.7) is not actually a distribution function to measure in the relative entropy. The problem can be solved by instead considering the spectral representation of the random process $q(t)$, from the *theory of spectral representation* of stationary random fields [82]. It is proved by Khinchin's formula [82], that if the autocorrelation function $\mathcal{R}(t)$ makes smooth and rapid-decay, a positive definite matrix $E(\lambda) > 0$ can be constructed so that the *spectral representations* of the autocorrelation $\mathcal{R}(t)$ and stationary process q become

$$\mathcal{R}(t) = \int_{-\infty}^{\infty} e^{i\lambda t} dF(\lambda), \quad q(t) = \int_{-\infty}^{\infty} e^{i\lambda t} \hat{Z}(d\lambda), \tag{6.8}$$

where the spectral random measure $\hat{Z}(d\lambda)$ has independent increments and energy spectrum measured by $dF(\lambda) = E(\lambda) d\lambda = \mathbb{E}|\hat{Z}(d\lambda)\hat{Z}^*(d\lambda)|$. Applying the theory for spectral representation of stationary processes, we find the one-to-one correspondence between the autocorrelation function $\mathcal{R}(t)$ and positive-definite energy spectra $E(\lambda)$, together with the spectral representation $\hat{Z}(d\lambda)$ of the stochastic process $q(t)$. We seek a spectral representation about the autocorrelation function like

$$\mathcal{P}(E(\lambda), E_M(\lambda)) = \int \mathcal{D}\left(E(\lambda) E_M(\lambda)^{-1}\right) d\lambda, \tag{6.9}$$

where $\mathcal{D}(x) \equiv -\log \det x + \text{tr} x - 2$ is the Gaussian relative entropy with a zero mean state. And since here we only concentrate on the leading order statistics (that is, mean and variance), thus this representation is enough. We can find the optimal model parameter $\boldsymbol{\theta}_* = (d_M, \omega_M)$ by minimizing the information metric defined in (6.9)

$$\mathcal{P}(E(\lambda), E_M(\lambda, \boldsymbol{\theta}_*)) = \min_{\boldsymbol{\theta}} \mathcal{P}(E(\lambda), E_M(\lambda, \boldsymbol{\theta})). \tag{6.10}$$

Note that in the reduced-order model in (6.4), the dynamics in each mode is set to be simple and linear, thus the model is efficient to run and even affordable for ensemble method to run a group of particles to capture the statistics in important spectral modes. The detailed description of the above strategy can be found in [66, 69].

6.2.2 Prediction of extreme events in tracers in the baroclinic turbulence

We test the reduced-order models described in the framework of the two-layer baroclinic model (2.9e). In numerical simulations, the true statistics is calculated by a pseudo-spectra code by resolving the two-layer equations with 64 spectral modes zonally and meridionally, corresponding to $128 \times 128 \times 2$ grid points in total. The time integration is through the standard 4th-order Runge-Kutta methods. The tracer field is simulated directly using the two-layer flow solution. In the reduced-order models, we only compute the large truncation $|\mathbf{k}| \le M = 10$ in largest scale modes, compared with the true system resolution $|\mathbf{k}| \le N = 64$.
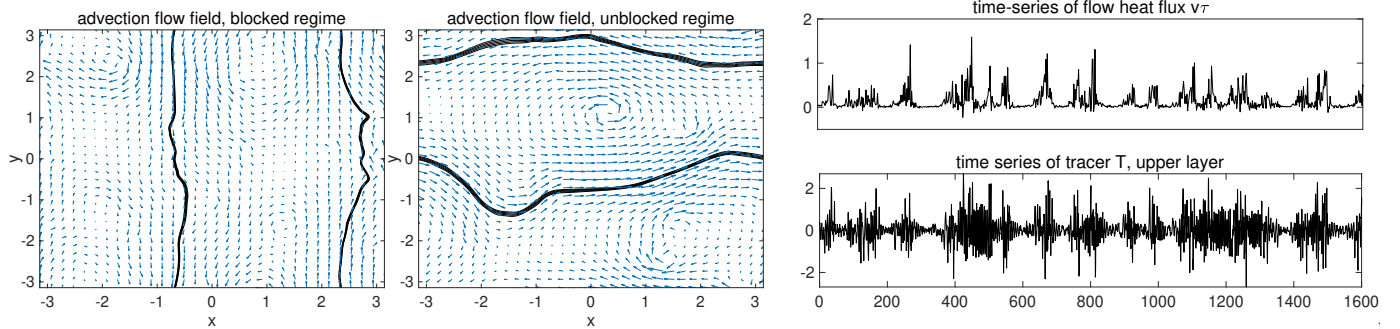
Figure 6.1: Illustration about tracer intermittency with heat flux. The first row is the snapshots of the flow field with blocked and unblocked regime. The following parts show typical time-series for both the heat flux and scalar passive tracer.

As a typical example, Figure 6.1 displays the representative flow and tracer structures from direction numerical simulations. The time-series of the heat flux $H_f = \int v\tau = \int \psi_x \tau$ illustrate the heat transfer mechanism. In the unblocked regime with strong zonal flow, the meridional heat flux is suppressed; while in the blocked regime strong meridional heat flux can be observed showing a strong meridional transport of the heat. The source of intermittency in passive scalar tracer is described qualitatively in [7] under an elementary model. Strong tracer intermittent bursts are always corresponding to the strong meridional heat transport in blocked regime leading to high mixing rate in tracer modes; the quite regime with little meridional heat flux in the unblocked regime also shows little intermittency of the tracer field in small amplitude.

The above on and off intermittent mechanism detailed in [7, 52] explains the turbulent mixing and intermittency via streamlines blocking and opening through simple elementary model with no instability and turbulence, while similar phenomena are also observed in the numerical simulations through much more complex two-layer baroclinic model in turbulence here. Even though simple and qualitative, the intuitive reasoning hints that the first two most energetic leading modes (0,1) and (1,0) which represent the competitive unblocked and blocked regime might be crucial for modeling the intermittent structures in the tracer field.

Still, the two-layer turbulent model includes much more complicated non-Gaussian nonlinear features. So next we test the performance with combination of the reduced-order models (6.4) and (6.5), and check how the tuning procedure in training phase can improve the imperfect model prediction skill. Figure 6.2 plots the time-series and PDFs of the leading tracer modes with strong intermittent structures. First qualitatively, the reduced model captures the occurrence of extreme events with much less computation cost. Next quantitatively in the PDFs, the fat tails representing the more frequent occurrence of extreme values are also captured from the reduced order model. Notice here in the reduced-order approximation, only the largest scale modes $|\mathbf{k}| \leq 10$ are resolved compared with the full model with a resolution of 128 grid points along each horizontal direction. The model efficiency can be effectively improved by adopting the low-order model. A complete comparison of the skills of the reduced-order stochastic model for the recovery of tracer energy spectra, eddy diffusivity, and various fat-tailed distributions in different ocean/atmosphere regimes is shown in [69].

7 Summarizing Discussions

Linear and nonlinear statistical response theory provides an effective tool to analyze the various problems and challenges in high-dimensional turbulent dynamical systems [45, 37, 81, 39]. In this paper, we summarize several useful perspectives of the linear and nonlinear response theory with applications to sensitivity analysis, uncertainty quantification, and control of complex turbulent systems [45, 39, 54, 68]. The effectiveness of the various strategies described in the main text are displayed under a hierarchy of simplified prototype models ranging from exactly solvable equations to geophysical turbulence with anisotropic dynamics.

We first provide a brief introduction to the general statistical response theory in Section 2. The practical skills in predicting multiscale variability in mean and variance using the linear response operators with various approximation strategies are discussed in Section 3 using the two-layer L-96 model showing nontrivial nonlinear responses. The accuracy with the different equilibrium statistical approximations is calibrated under the unbiased information metric [40]. Already under this simple framework, it shows the importance of considering the higher order non-Gaussian statistics even for the accurate prediction in the second order variance responses. The extent of the prediction skill in the linear response
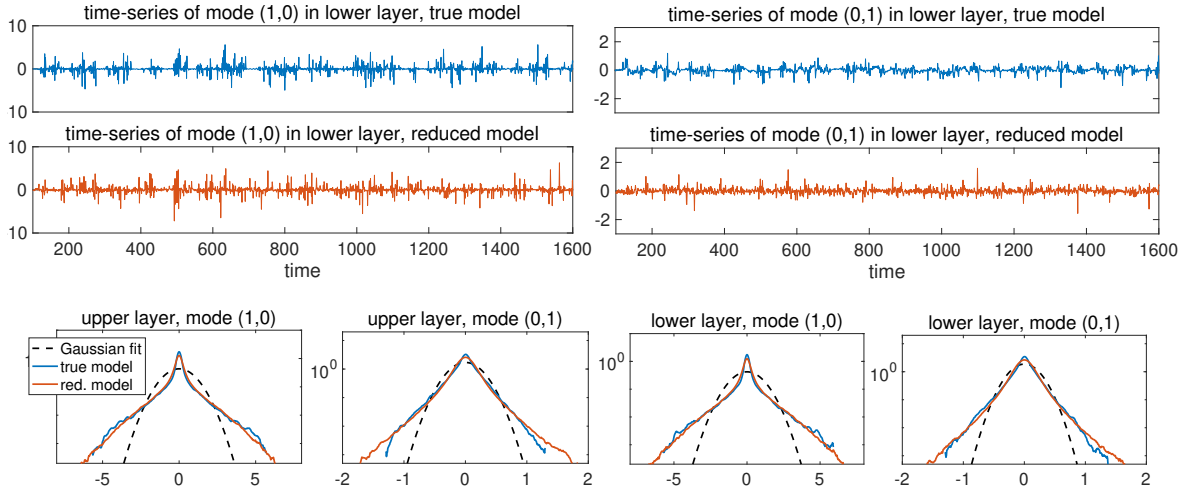
Figure 6.2: Prediction about tracer intermittency using stochastic reduced order model. The left panel is the time-series for the first two leading modes (1,0) and (0,1) between true model and reduced model results; the right panel compares the PDFs in the first four modes between the truth in blue and reduced model prediction in red with the Gaussian fit in dashed black lines.

theory is limited in the small perturbation regime. This shortcoming becomes more obvious in the anisotropic barotropic turbulence in Section 4 where the nonlinear response to the external forcing perturbations is particularly strong.

A systematic information-theoretic framework [45, 39, 49] is shown effective to improve the prediction skill and capture the nonlinear response trend. Without dependence on the specific perturbation form, a statistical model reduction strategy in general can be applied to any turbulent dynamic systems with model error for predicting any perturbed responses. It is required for the models to recover the crucial features of the natural system in statistical equilibrium for climate fidelity, and improve the model sensitivity in response to various external perturbations like climate change and mitigation scenarios. Linear response theory, in turn, provides important guideline for the tuning of optimal imperfect model parameters in the training phase in a systematic fashion. The validity of the reduced-order statistical models is displayed first in the simplest three-dimensional triad model for characterizing the typical features in the strategy, and then to the more complex topographic barotropic flows including multiscale flow interactions with detailed investigation in Section 4. The model error is effective reduced by combining the linear response theory with the efficient information theory calibration. Besides the turbulent flow field, the dynamics of passive tracers advected by the turbulent flow also contain many distinctive features, such as, the occurrence of extreme events characterized by fat-tails in the tracer density distributions. The same model reduction idea is applied to the construction of stochastic models [69, 66] aiming to capture such extreme events. In Section 6, the reduced-order stochastic model displays uniform high skill in capturing fat-tails in the leading resolved modes using the complex two-layer baroclinic model.

The statistical response theory also displays a promising role in the development of effective control of high-dimensional dynamical systems [54, 55]. Instead of a direct control on the state variables in a high-dimensional phase space, the simple scalar dynamical equation makes it possible for the control of total statistical energy in an efficient way. Using the total statistical energy equation [54] avoids treating the complicated higher order nonlinear interactions with instabilities. The statistical responses in the mean subject to external forcing is approximated using linear response theory without the need to run the explicit model. The control performance is illustrated using the same topographic barotropic model in Section 5. Despite the model errors introduced through the leading order expansion in both the statistical equation and linear prediction in mean response, the statistical control methods have uniform robust skill for controlling the homogeneously and inhomogeneously perturbed system in the same fashion. Furthermore this statistical control strategy shows potential for extremely high dimensional problems in combination with turbulent flows and passive turbulence.

Acknowledgement

References

[1] Rafail V Abramov and Andrew J Majda. Blended response algorithms for linear fluctuation-dissipation for complex nonlinear dynamical systems. *Nonlinearity*, 20(12):2793, 2007.

[2] Rafail V Abramov and Andrew J Majda. Low-frequency climate response of quasigeostrophic wind-driven ocean circulation. *Journal of Physical Oceanography*, 42(2):243–260, 2012.

[3] Brian DO Anderson and John B Moore. *Linear optimal control*, volume 197. Prentice-Hall Englewood Cliffs, NJ, 1971.

[4] Marco Avellaneda and Andrew J Majda. Simple examples with features of renormalization for turbulent transport. *Philosophical Transactions of the Royal Society of London A: Mathematical, Physical and Engineering Sciences*, 346(1679):205–233, 1994.

[5] Martino Bardi and Italo Capuzzo-Dolcetta. *Optimal control and viscosity solutions of Hamilton-Jacobi-Bellman equations*. Springer Science & Business Media, 2008.

[6] Thomas L Bell. Climate sensitivity from fluctuation dissipation: Some simple model tests. *Journal of the Atmospheric Sciences*, 37(8):1700–1707, 1980.

[7] A Bourlioux and AJ Majda. Elementary models with probability distribution function intermittency for passive scalars with a mean gradient. *Physics of Fluids (1994-present)*, 14(2):881–897, 2002.

[8] Steven L Brunton and Bernd R Noack. Closed-loop turbulence control: progress and challenges. *Applied Mechanics Reviews*, 67(5):050801, 2015.

[9] Kenneth P Burnham and David Anderson. Model selection and multi-model inference. *A Pratical informatio-theoric approch. Sringer*, 2003.

[10] George F Carnevale and Jorgen S Frederiksen. Nonlinear stability and statistical mechanics of flow over topography. *Journal of Fluid Mechanics*, 175:157–181, 1987.

[11] GF Carnevale, M Falcioni, S Isola, R Purini, and Angelo Vulpiani. Fluctuation-response relations in systems with chaotic behavior. *Physics of Fluids A: Fluid Dynamics (1989-1993)*, 3(9):2247–2254, 1991.

[12] N Chen and AJ Majda. Predicting the real-time multivariate madden–julian oscillation index through a low-order nonlinear stochastic model. *Monthly Weather Review*, 143(6):2148–2169, 2015.

[13] N Chen, AJ Majda, and D Giannakis. Predicting the cloud patterns of the Madden-Julian oscillation through a low-order nonlinear stochastic model. *Geophysical Research Letters*, 41:5612–5619, 2014.

[14] Nan Chen and Andrew Majda. Conditional gaussian systems for multiscale nonlinear stochastic systems: Prediction, state estimation and uncertainty quantification. *Entropy*, 20(7):509, 2018.

[15] Nan Chen and Andrew J Majda. Beating the curse of dimension with accurate statistics for the fokker–planck equation in complex turbulent systems. *Proceedings of the National Academy of Sciences*, 114(49):12864–12869, 2017.

[16] Yat Tin Chow, Jérôme Darbon, Stanley Osher, and Wotao Yin. Algorithm for overcoming the curse of dimensionality for time-dependent non-convex Hamilton–Jacobi equations arising from optimal control and differential games problems. *Journal of Scientific Computing*, pages 1–27, 2016.

[17] Timothy DelSole and Jagadish Shukla. Model fidelity versus skill in seasonal forecasting. *Journal of Climate*, 23(18):4794–4806, 2010.

[18] Lawrence C Evans. An introduction to mathematical optimal control theory. *Lecture Notes, University of California, Department of Mathematics, Berkeley*, 2005.

[19] Dargan MW Frierson. Robust increases in midlatitude static stability in simulations of global warming. *Geophysical research letters*, 33(24), 2006.

[20] Uriel Frisch. *Turbulence: the legacy of AN Kolmogorov*. Cambridge university press, 1995.

[21] Boris Gershgorin and Andrew J Majda. A test model for fluctuation–dissipation theorems with time-periodic statistics. *Physica D: Nonlinear Phenomena*, 239(17):1741–1757, 2010.

[22] Boris Gershgorin and Andrew J Majda. Quantifying uncertainty for climate change and long-range forecasting scenarios with model errors. Part I: Gaussian models. *Journal of Climate*, 25(13):4523–4548, 2012.

[23] A Gettelman, JE Kay, and KM Shell. The evolution of climate sensitivity and climate feedbacks in the community atmosphere model. *Journal of Climate*, 25(5):1453–1469, 2012.

[24] Alexander Gluhovsky and Ernest Agee. An interpretation of atmospheric low-order models. *Journal of the atmospheric sciences*, 54(6):768–773, 1997.

[25] Georg A Gottwald, JP Wormell, and Jeroen Wouters. On spurious detection of linear response and misuse of the fluctuation–dissipation theorem in finite time series. *Physica D: Nonlinear Phenomena*, 331:89–101, 2016.

[26] Andrey Gritsun and Grant Branstator. Climate response using a three-dimensional operator based on the fluctuation-dissipation theorem. *Journal of the atmospheric sciences*, 64(7):2558–2575, 2007.

[27] Andrey Gritsun, Grant Branstator, and Andrew Majda. Climate response of linear and quadratic functionals using the fluctuation-dissipation theorem. *Journal of the Atmospheric Sciences*, 65(9):2824–2841, 2008.

[28] Marcus J Grote, Andrew J Majda, and C Grotta Ragazzo. Dynamic mean flow and small-scale interaction through topographic stress. *Journal of Nonlinear Science*, 9(1):89–130, 1999.

[29] Martin Hairer and Andrew J Majda. A simple framework to justify linear response theory. *Nonlinearity*, 23(4):909, 2010.

[30] John Harlim. *Data-driven computational methods: parameter and operator estimations*. Cambridge University Press, 2018.

[31] Edwin T Jaynes. Information theory and statistical mechanics. *Physical review*, 106(4):620, 1957.

[32] Richard Kleeman, Andrew J Majda, and Ilya Timofeyev. Quantifying predictability in a model with statistical features of the atmosphere. *Proceedings of the National Academy of Sciences*, 99(24):15291–15296, 2002.

[33] Solomon Kullback and Richard A Leibler. On information and sufficiency. *The annals of mathematical statistics*, pages 79–86, 1951.

[34] Y Lee and AJ Majda. Multiscale data assimilation and prediction using clustered particle filters. *J Comput Phys, in press*, 2017.

[35] CE Leith. Climate response and fluctuation dissipation. *Journal of the Atmospheric Sciences*, 32(10):2022–2026, 1975.

[36] Edward N Lorenz. Predictability: A problem partly solved. In *Proc. Seminar on predictability*, volume 1, 1996.

[37] Nicholas J Lutsko, Isaac M Held, and Pablo Zurita-Gotor. Applying the fluctuation–dissipation theorem to a two-layer model of quasigeostrophic turbulence. *Journal of the Atmospheric Sciences*, 72(8):3161–3177, 2015.

[38] Douglas G MacMartin, Ben Kravitz, David W Keith, and Andrew Jarvis. Dynamics of the coupled human–climate system resulting from closed-loop control of solar geoengineering. *Climate dynamics*, 43(1-2):243–258, 2014.

[39] A. Majda and D. Qi. Strategies for reduced-order models for predicting the statistical responses and uncertainty quantification in complex turbulent dynamical systems. *SIAM Review*, 60(3):491–549, 2018.

[40] Andrew Majda, Rafail V Abramov, and Marcus J Grote. *Information theory and stochastics for multiscale nonlinear systems*, volume 25. American Mathematical Soc., 2005.

[41] Andrew Majda and Nan Chen. Model error, information barriers, state estimation and prediction in complex multiscale systems. *Entropy*, 20(9):644, 2018.

[42] Andrew Majda and Xiaoming Wang. *Nonlinear dynamics and statistical theories for basic geophysical flows*. Cambridge University Press, 2006.

[43] Andrew Majda and Xiaoming Wang. Linear response theory for statistical ensembles in complex systems with time-periodic forcing. *Communications in Mathematical Sciences*, 8(1):145–172, 2010.

[44] Andrew J Majda. Statistical energy conservation principle for inhomogeneous turbulent dynamical systems. *Proceedings of the National Academy of Sciences*, 112(29):8937–8941, 2015.

[45] Andrew J Majda. *Introduction to Turbulent Dynamical Systems in Complex Systems*. Springer, 2016.

[46] Andrew J Majda, Rafail Abramov, and Boris Gershgorin. High skill in low-frequency climate response through fluctuation dissipation theorems despite structural instability. *Proceedings of the National Academy of Sciences*, 107(2):581–586, 2010.

[47] Andrew J Majda and Michal Branicki. Lessons in uncertainty quantification for turbulent dynamical systems. *Discrete Cont. Dyn. Systems*, 32(9):3133–3221, 2012.

[48] Andrew J Majda, Christian Franzke, and Daan Crommelin. Normal forms for reduced stochastic climate models. *Proceedings of the National Academy of Sciences*, 106(10):3649–3653, 2009.

[49] Andrew J Majda and Boris Gershgorin. Improving model fidelity and sensitivity for complex systems through empirical information theory. *Proceedings of the National Academy of Sciences*, 108(25):10044–10049, 2011.

[50] Andrew J Majda and Boris Gershgorin. Link between statistical equilibrium fidelity and forecasting skill for complex systems with model error. *Proceedings of the National Academy of Sciences*, 108(31):12599–12604, 2011.

[51] Andrew J Majda, Boris Gershgorin, and Yuan Yuan. Low-frequency climate response and fluctuation-dissipation theorems: theory and practice. *Journal of the Atmospheric Sciences*, 67(4):1186–1201, 2010.

[52] Andrew J Majda and Peter R Kramer. Simplified models for turbulent diffusion: theory, numerical modelling, and physical phenomena. *Physics reports*, 314(4):237–574, 1999.

[53] Andrew J Majda and Di Qi. Improving prediction skill of imperfect turbulent models through statistical response and information theory. *Journal of Nonlinear Science*, 26(1):233–285, 2016.

[54] Andrew J Majda and Di Qi. Effective control of complex turbulent dynamical systems through statistical functionals. *Proceedings of the National Academy of Sciences*, 114(22):5571–5576, 2017.

[55] Andrew J Majda and Di Qi. Using statistical functionals for effective control of inhomogeneous complex turbulent dynamical systems. *Physica D: Nonlinear Phenomena*, 392:34–56, 2019.

[56] Andrew J Majda and Xin T Tong. Ergodicity of truncated stochastic Navier-Stokes with deterministic forcing and dispersion. *Journal of Nonlinear Science*, 26(5):1483–1506, 2015.

[57] Andrew J Majda and Xin T Tong. Intermittency in turbulent diffusion models with a mean gradient. *Nonlinearity*, 28(11):4171–4208, 2015.

[58] Andrew J Majda and Xin T Tong. Simple nonlinear models with rigorous extreme events and heavy tails. *Nonlinearity*, 32(5):1641, 2019.

[59] Umberto Marini Bettolo Marconi, Andrea Puglisi, Lamberto Rondoni, and Angelo Vulpiani. Fluctuation–dissipation: response theory in statistical physics. *Physics reports*, 461(4):111–195, 2008.

[60] Mustafa A Mohamad and Andrew J Majda. Recovering the eulerian energy spectrum from noisy lagrangian tracers. 2018.

[61] Mustafa A Mohamad and Themistoklis P Sapsis. Probabilistic description of extreme events in intermittently unstable dynamical systems excited by correlated stochastic processes. *SIAM/ASA Journal on Uncertainty Quantification*, 3(1):709–736, 2015.

[62] J David Neelin, Benjamin R Lintner, Baijun Tian, Qinbin Li, Li Zhang, Prabir K Patra, Moustafa T Chahine, and Samuel N Stechmann. Long tails in deep columns of natural and anthropogenic tropospheric tracers. *Geophysical Research Letters*, 37(5), 2010.

[63] Dwight Roy Nicholson. *Introduction to plasma theory.* Cambridge Univ Press, 1983.

[64] Tim Palmer, Paul Williams, and Paul Williams. *Stochastic physics and climate modelling.* Cambridge University Press Cambridge, UK, 2010.

[65] Stephen B Pope. *Turbulent flows.* IOP Publishing, Bristol, 2001.

[66] Di Qi and Andrew J Majda. Predicting fat-tailed intermittent probability distributions in passive scalar turbulence with imperfect models through empirical information theory. *Comm. Math. Sci*, 14(6):1687–1722, 2015.

[67] Di Qi and Andrew J Majda. Low-dimensional reduced-order models for statistical response and uncertainty quantification: two-layer baroclinic turbulence. *Journal of the Atmospheric Sciences*, 73(12):4609–4639, 2016.

[68] Di Qi and Andrew J Majda. Low-dimensional reduced-order models for statistical response and uncertainty quantification: Barotropic turbulence with topography. *Physica D: Nonlinear Phenomena*, 343:7–27, 2017.

[69] Di Qi and Andrew J Majda. Predicting extreme events for passive scalar turbulence in two-layer baroclinic flows through reduced-order stochastic models. *Commun Math Sci*, 16:17–51, 2018.

[70] Di Qi and Andrew J Majda. Rigorous statistical bounds in uncertainty quantification for one-layer turbulent geophysical flows. *Journal of Nonlinear Science*, 28:1709–1761, 2018.

[71] Aaditya V Rangan, Louis Tao, Gregor Kovacic, and David Cai. Multiscale modeling of the primary visual cortex. *IEEE Engineering in Medicine and Biology Magazine*, 28(3):19–24, 2009.

[72] Rick Salmon. *Lectures on geophysical fluid dynamics.* Oxford University Press, 1998.

[73] Themistoklis P Sapsis. Attractor local dimensionality, nonlinear energy transfers and finite-time instabilities in unstable dynamical systems with applications to two-dimensional fluid flows. *Proceedings of the Royal Society A: Mathematical, Physical and Engineering Sciences*, 469(2153):20120550, 2013.

[74] Themistoklis P Sapsis and Andrew J Majda. A statistically accurate modified quasilinear gaussian closure for uncertainty quantification in turbulent dynamical systems. *Physica D: Nonlinear Phenomena*, 252:34–45, 2013.

[75] K Shafer Smith. Tracer transport along and across coherent jets in two-dimensional turbulent flow. *Journal of Fluid Mechanics*, 544:133–142, 2005.

[76] Andrew F Thompson and William R Young. Two-layer baroclinic eddy heat fluxes: Zonal flows and energy balance. *Journal of the Atmospheric Sciences*, 64(9):3214–3231, 2007.

[77] Geoffrey K Vallis. *Atmospheric and oceanic fluid dynamics: Fundamentals and large-scale circulation.* Cambridge University Press, 2006.

[78] Eric Vanden Eijnden. Non-gaussian invariant measures for the Majda model of decaying turbulent transport. *Communications on Pure and Applied Mathematics*, 54(9):1146–1167, 2001.

[79] Eric R Weeks, Yudong Tian, JS Urbach, Kayo Ide, Harry L Swinney, and Michael Ghil. Transitions between blocked and zonal flows in a rotating annulus with topography. *Science*, 278(5343):1598–1601, 1997.

[80] David Williams and David Williams. *Weighing the odds: a course in probability and statistics*, volume 3. Springer, 2001.

[81] Caroline L Wormell and Georg A Gottwald. On the validity of linear response theory in high-dimensional deterministic dynamical systems. *Journal of Statistical Physics*, 172(6):1479–1498, 2018.

[82] Akiva M Yaglom. *An introduction to the theory of stationary random functions.* Courier Corporation, 2004.

[83] Pablo Zurita-Gotor, Javier Blanco-Fuentes, and Edwin P Gerber. The impact of baroclinic eddy feedback on the persistence of jet variability in the two-layer model. *Journal of the Atmospheric Sciences*, 71(1):410–429, 2014.